

Interactive comment on “Spatio-temporal controls of C-N-P dynamics across headwater catchments of a temperate agricultural region from public data analysis” by Stella Guillemot et al.

2nd revision - Reply to Anonymous Referee #1

The response to the general comment is developed in the specific questions, particularly 3 and 6.

1. *L55: Homogenization of formerly (naturally) heterogeneous catchments is argued to be the main reason for nitrate chemostatic behavior and thus purely transport-limited nitrate exports. This does not fit to your description of homogeneity as a characteristic of natural catchments.*

The generalization of the drivers from C to C, N and P is mainly due to human pressure which could induce internal storage, and therefore, purely transport-limited nitrate exports. We stress now on pressure, rather than on homogeneity, for such generalization.

2. *L66 and L87: You boil down seasonality to a hydrological control (controlling other biogeochemical processes). What about light and temperature. In-stream ecosystems but also shallow near stream systems may be also be seasonally controlled by that.*

Light and temperature are now mentioned. Investigations on the effect of light and temperature on C, N and P concentrations are poor, because they really vary along the stream. Temperature does not vary a lot over Brittany, and light cannot easily be captured by simple indicators.

3. *L103: This sentence does not make sense for me.*

Line suppressed.

4. *L181ff: For me this is still not resolved and need to be explicitly mentioned here. By GAM you cannot analyze catchments without seasonality. Your SI metric thus does not cover the whole range of analysed catchments. If you want it like that, its ok. But you need to mention it.*

A sentence added. “GAM provides SI metrics on seasonality, which can be easily linked with different geographical variables. However, it cannot take into account catchments without seasonality.”

5. *Table 1: You added the information on the Topo_i. I just don't see the point why you don't use the established name "topographic wetness index" here. Moreover it is not clear how you derive one value for the entire catchment. Usually the Beven-Kirkby approach derives this for each grid cell of the DEM. Finally, the unit seems to be wrong: log[ha]? Note that Beven and Kirkby use the local slope in radian not %.*

Corrected. Indeed, it is preferable to use the name “average topographic wetness index” (meanTWI) rather than “downstream topographic index” (Topo_i), even if the usual TWI in the literature takes into account the local slope rather than the downstream slope.

We derived the value for each cell of the DEM grid according to the Beven-Kirkby approach:

$TWI = \log \frac{\alpha}{\tan \beta}$. Where α is the drainage area (ha) and β is the downstream slope (%) (Merot et al., 2003). Then we averaged the values of each cell present on the drained surface to obtain a "meanTWI" value for the entire watershed, expressed in log(Ha).

6. *L205: Again I ask for a bit more words on the idea of the PCA. Tell the reader why you use this technique, what it can tell you and what are potential drawbacks that have to be kept in mind. For instance, PCA is a linear method and explained variance may be misleading when relations between the elements are non-linear (e.g. the power law that Taylor and Townsend propose for C:N). Your rank correlation acknowledge that but this, again is not mentioned. It would help the paper elaborating on this to not leave the impression you randomly chose you methods which surely is not the case.*

A sentence added. "PCA was chosen, despite it assumes linear relationships between variables, because it provides a graphical representation of correlations between variables or groups of variables and their contributions the variance."

7. *L233: I criticized the use of PCA in the first review. Now you moved it to the Supplement which does not solve the issue but rather complicates it. If you want to use it, it's ok but needs to be justified (see above comment) and then properly used in the main manuscript.*

See the sentence added L205. Add the results of PCA include again in the main manuscript.

8. *L237: This link to S4b is for C50 only - should be mentioned here. Wouldn't it make sense and be easier to have a correlation matrix for all concentration metrics across all constituents in the SI?*

It's done. We added the precision on C50 and the S8 supplement reference (correlation matrix).

9. *L242: Here you use SI the first time in the results. At this point it would be good to mention that this does not incorporate all catchments and give the number of cases?*

A sentence was added "..., calculated on the catchments for which a GAM can be fitted, i.e. presenting a seasonal feature,..."

10. *L295f: If the classification of "in-phase" and "out-of-phase" refers to van Meter et al. 2019, it would be fair to mention it.*

Reference added.

11. *L414: The meaning of a synchronization of a contribution with maximum flow is not fully clear to me.*

Definition added.

12. *L415: Redox-processes may be mentioned explicitly as this seems solely refer to assimilation.*

"Redox-processes" added.

13. *L422: I know what you mean but expression is not fully transporting that. Maybe: "decrease NO3 concentration more in shallower and younger groundwater than in deeper, older groundwater"?*

Corrected.

14. *L495ff: Without explicitly mentioning it the entire monitoring and management implications are boiled down to the discussion of C:N ratios which haven't been presented in the results at all. and actually no implications are mentioned in this section. I suggest to broaden the view here a bit and share with the reader how your result may influence water quality management and monitoring design.*

Few sentences on consequences on water quality management and monitoring design have been added.

“However, we can stress that monitoring C-N and P is important as each of these elements can follow a specific pattern, even in neighboring catchments. Yet, these three basic elements are not always analyzed in water quality monitoring. Therefore, sample points for which monitoring associate these three elements have to be preserve for a long term monitoring. They will be necessary to further investigate their variations in relation with geomorphological and climate conditions. In this paper, we used inter-annual mean values for DOC, NO₃ and SRP loads to establish the spatial variability and the seasonal patterns across headwater catchments. Because we demonstrated that seasonality index (SI) and flow flashiness (W₂) are linked, our results can be used to classify non-monitored catchments as a function of their potential load flashiness. Flow flashiness (W₂) combined with SI or the slope of C-Q relationships for high flows, could be employed for a sampling monitoring design to improve annual or seasonal load estimations for the most contributive catchments (Moatar et al, 2020). Yet, other issues, such as the assessment of eutrophication risk for some lakes, estuaries or bays around the peninsula would require more frequent sampling especially for SRP. “

Interactive comment on “Spatio-temporal controls of C-N-P dynamics across headwater catchments of a temperate agricultural region from public data analysis” by Stella Guillemot et al.

2nd revision - Reply to Anonymous Referee #2

The authors have done a thorough job of addressing reviewer comments and revising this paper.

I appreciate the clarification provided on statistical methods and the potential challenges to implementing an expanded GAM model. As the authors suggest in their responses, the approach to statistical analysis being altered is unlikely to change the over conclusions of the descriptive study. Suggestions of an expanded GAM model based on reading the first draft of the manuscript were mainly out of interest as to whether an alternative statistical approach would be complementary in simplifying or integrating presentation of some of the results and exploring interactions between geographic variables, hydrology, and concentration. As currently presented the results clearly highlight seasonality very well. Also, where discharge and concentrations follow similar seasonality it is visually evident through the GAM results. However, I do wonder if there might still be some room to explore whether the geographic variables influencing seasonality of discharge are the same as those for concentrations. This could just be a simple addition of correlations between discharge seasonality metrics and geographic variables to Table 3. That would allow for a test of whether the controls are similar

Spatio-temporal controls of C-N-P dynamics across headwater catchments of a temperate agricultural region from public data analysis

Stella Guillemot^{1,2}, Ophelie Fovet¹, Chantal Gascuel-Oudou¹, Gérard Gruau³, Antoine Casquin¹, Florence Curie², Camille Minaudo⁴, Laurent Strohmenger¹, and Florentina Moatar^{5,2}

¹INRAE, AGROCAMPUS OUEST/INSTITUT AGRO, UMR SAS, 35000 Rennes, France

²Université de Tours, EA 6293 GÉHCO, 37200 Tours, France

³OSUR, Geosciences Rennes, CNRS, Université Rennes 1, 35000 Rennes, France

⁴EPFL, Physics of Aquatic Systems Laboratory, 1015 Lausanne, Switzerland

10 ⁵INRAE, RIVERLY, 69625 Villeurbanne, France

Correspondence to: Ophelie Fovet (ophelie.fovet@inrae.fr)

Abstract. Characterizing and understanding spatial variability in water quality for a variety of chemical elements is an issue for present and future water resource management. However, most studies of spatial variability in water quality focus on a single element and rarely consider headwater catchments. Moreover, they assess few catchments and focus on annual means without considering seasonal variations. To overcome these limitations, we studied spatial variability and seasonal variation in dissolved C, N, and P concentrations at the scale of an intensively farmed region of France (Brittany). We analyzed 185 headwater catchments (from 5-179 km²) for which 10-year time series of monthly concentrations and daily stream flow were available from public databases. We calculated interannual loads, concentration percentiles, and seasonal metrics for each element to assess their spatial patterns and correlations. We then performed rank correlation analyses between water quality, human pressures, and soil and climate features. Results show that nitrate (NO₃) concentrations increased with increasing agricultural pressures and base flow contribution; dissolved organic carbon (DOC) concentrations decreased with increasing rainfall, base flow contribution, and topography; and soluble reactive phosphorus (SRP) concentrations showed weaker positive correlations with diffuse and point sources, rainfall and topography. An opposite pattern was found between DOC and NO₃: spatially, between their median concentrations, and temporally, according to their seasonal cycles. In addition, the quality of annual maximum NO₃ concentration was in-phase with maximum flow when the base flow index was low, but this synchrony disappeared when flow flashiness was lower. These DOC-NO₃ seasonal cycle types were related to the mixing of flowpaths combined with the spatial variability of their respective sources and to local biogeochemical processes. The annual maximum SRP concentration occurred during the low-flow period in nearly all catchments. This likely resulted from the dominance of P point sources. The approach shows that despite the relatively low frequency of public water quality data, such databases can provide consistent pictures of the spatio-temporal variability of water quality and of its drivers as soon as they contain a large number of catchments to compare and a sufficient length of concentration time series.

1 Introduction

As a condition for human health, food production, and ecosystem functions, water quality is recognized as “one of the main challenges of the 21st century” (FAO and WWC, 2015; UNESCO, 2015), and potential impacts of climate change on water quality are even more challenging (Whitehead et al., 2009). To better estimate and reduce human impact on water quality, water scientists are expected to provide integrated understanding of multiple pollutants (Cosgrove and Loucks, 2015). Eutrophication risks (Dodds and Smith, 2016) are considered the main factors that decrease the quality of surface water, according to objectives set by the European Union Water Framework Directive. Mitigating the problem of eutrophication involves considering at least the three major elements: carbon (C), nitrogen (N), and phosphorus (P) (Le Moal et al., 2019). In addition, the quality of headwater catchments have been studied less than large rivers (Bishop et al., 2008), despite their influence on downstream water quality (Alexander et al., 2007; Barnes and Raymond, 2010; Bol et al., 2018) and higher spatial variability in their concentrations (Abbott et al., 2018a; Temnerud and Bishop, 2005). One reason for this is that most water quality monitoring networks coincide with the location of drinking-water production facilities, which explains why they focus on large rivers. Nonetheless, investigating spatial variability in upstream water quality is relevant for understanding what causes it to degrade, targeting locations with the greatest disturbances, and identifying which remediation policies would be most cost effective.

In non-agricultural headwater catchments, spatial variability in dissolved organic C (DOC) concentrations in streams has been related to topography, wetland coverage, and soil properties such as clay content or pH (Andersson and Nyberg, 2008; Brooks et al., 1999; Creed et al., 2008; Hytteborn et al., 2015; Musolff et al., 2018; Temnerud and Bishop, 2005; Zarnetske et al., 2018). Stream DOC concentrations and composition in agricultural and urbanized areas also generally differ greatly from those in semi-natural or pristine catchments (Graeber et al., 2012; Gücker et al., 2016). Over large gradients of human impact (e.g. from undisturbed to urban catchments), the cover of agricultural and urban land uses often appears as a key factor that explains differences in stream chemistry of C, N, and P species (e.g. Barnes and Raymond, 2010; Edwards et al., 2000; Mutema et al., 2015) and even silica (Onderka et al., 2012). Conversely, in ~~mostly undisturbed catchments more homogeneous catchments—~~ ~~e.g. mostly undisturbed~~ (Mengistu et al., 2014) or ~~mostly rural where human pressure are low~~ (Heppell et al., 2017; Lintern et al., 2018)— “natural” controls such as topography, geology, and flow paths are more frequently highlighted as the main factors that explain spatial variability in C, N and P.

Besides being spatially variable, C, N, and P concentrations also vary temporally. The variability of concentrations with flow has been described in several studies using concentration-flow relationships at event (Fasching et al., 2019) or inter-annual to long-term scales (Basu et al., 2010; 2011; Moatar et al., 2017). Concentrations also vary seasonally in streams and rivers (Aubert et al., 2013; Dawson et al., 2008; Duncan et al., 2015; Exner-Kittridge et al., 2016; Lambert et al., 2013), as does the composition of dissolved organic matter (Griffiths et al., 2011; Gücker et al., 2016). This seasonality can also be spatially structured. Several studies showed that the relative importance of catchment characteristics on water concentrations or loads varied by season because nutrient sources and biological and physico-chemical processes that influence nutrient mobilization

and transfer in catchments (e.g. vegetation uptake, in-stream biomass production, denitrification) changed with the hydrological, [light and temperature](#) conditions (Ågren et al., 2007; Fasching et al., 2016; Gardner and McGlynn, 2009). Some variability in seasonal patterns of dissolved C, N, and/or P concentrations among headwater catchments has been reported (e.g. Van Meter et al., 2019; Abbott et al., 2018b; Duncan et al., 2015; Martin et al., 2004). Identifying these patterns is relevant from a management viewpoint as they may indicate changes in the locations of C, N, or P sources or their transfer pathways.

Thus, to date, analysis of spatial variability in water quality at the headwater scale:

- 1) is usually restricted to one element, although multi-element approaches are becoming more frequent (Edwards et al., 2000; Heppell et al., 2017; Lintern et al., 2018; Mengistu et al., 2014; Mutema et al., 2015),
- 2) is particularly rare for headwater catchments with similar human pressures (e.g. intensive farming), despite the high variability in water quality sometimes observed among them (e.g. Thomas et al., 2014),
- 3) often uses mean annual values (concentration or load) to describe spatial variability in water quality among catchments, with little or no analysis of seasonal patterns despite their frequent occurrence (Van Meter et al., 2019; Abbott et al., 2018b; Liu et al., 2014; Halliday et al., 2012; Mullholland et al. 1997), and
- 4) is usually restricted to a few catchments: multiple-catchment studies on multiple elements are uncommon, despite their ability to identify dominant controlling factors better.

We studied the spatial variability and seasonal variation in water quality of 185 headwater catchments (from 5-179 km²) draining Brittany, an intensively farmed region of France. Our analysis focuses on dissolved C, N, and P concentrations as DOC, nitrate (NO₃), and soluble reactive P (SRP), respectively. We hypothesized that:

- 1) Human (i.e. rural and urban) pressures determine spatial variability in NO₃ and SRP concentrations (Preston et al., 2011; Melland et al., 2012; Dupas et al., 2015a; Kaushal et al., 2018), while soil and climate characteristics, [including light and temperature along the stream](#), determine that in DOC and possibly SRP (Lambert et al., 2013; Humbert et al., 2015; Gu et al., 2017).
- 2) Seasonal variations in water quality provide information about spatial variability in biogeochemical sources and/or reactivity in catchments as a function of changes in water pathways and are correlated in part with spatial variability in concentrations and loads.

We selected headwater catchments for which relevant time series of DOC, NO₃, and SRP concentrations and stream flow were available (10 years of consecutive data measured at least monthly). In addition to estimating interannual loads, we calculated concentration metrics for each element to assess the spatial variability and temporal variation in water quality. Generalized Additive Models (GAMs) were applied to the time series to highlight average patterns of seasonal variation. Correlations between the water quality metrics and the geological, soil, climatic, hydrological, land cover, and human pressure characteristics of the corresponding headwater catchments were evaluated using rank correlation analyses.

2 Materials and Methods

100 2.1 Study area

Brittany is a 27,208 km² region in western France. Its bedrock is composed mainly of a crystalline substratum dominated by granite and schist (Supplement S1b). Its topography is moderate, with elevation ranging from 0-330 m a.s.l. Its climate is temperate oceanic, with precipitation ranging from 531 mm.yr⁻¹ in the east to 1070 mm.yr⁻¹ on the western coasts (regional median of 723.0 mm.yr⁻¹) (Supplement S1a), and a mean annual temperature of 12°C. The regional hydrographic network is
105 dense, with a mean density of 1 km.km⁻². ~~Its intensive agriculture has a strong influence on land use and agri-food production.~~
Overall, 56.6% of the region was Utilized Agricultural Area (UAA) in 2017 (data from DREAL Bretagne, Brittany's Agency for Environment, Infrastructure, and Housing), which represented 6% of national UAA in 2016. Of total French production, Brittany produces 17.4% of milk and dairy products, 20% of pork products, and 17% of eggs and poultry (Brittany Chamber of Agriculture, 2016 data). At the canton (administrative district) scale, mean N and P surpluses are high and have high spatial
110 variability (standard deviation (SD)): 50.01 ± 26.59 kg N.ha⁻¹.yr⁻¹ and 22.52 ± 12.66 kg P.ha⁻¹.yr⁻¹ (Supplement S1e,f). The region has a population of ca 3.3 million inhabitants (data 2017), some scattered throughout the region, and some concentrated in a few cities and near the coasts (Supplement S1c,d).

2.2 Stream data selection and headwater characteristics

115 Water quality data consisted of time series of DOC, NO₃, and SRP concentrations, extracted from two public monitoring networks – OSUR (Loire-Brittany Water Agency, 554 sites) and HYDRE/BEA (DREAL Bretagne, ca. 1964 sites), measured for regulatory monitoring, regional contracts, or specific programs. Concentrations were measured from grab samples. Headwater catchments were selected according to the following two criteria: (i) independence, with no overlap of the drained areas of the water-quality stations selected, and (ii) availability of at least 80 measurements of DOC, NO₃, and SRP
120 concentrations at the same station (after removing outliers based on expert knowledge, i.e. values > 200 mg N.L⁻¹ or 5 g P.L⁻¹) over 10 calendar years (2007-2016). We selected 185 stations (83% and 17% from OSUR and HYDRE/BEA, respectively) (hereafter, “concentration (C) stations”), which had mean frequencies of 12, 14, and 11 analyses per year for DOC, NO₃, and SRP, respectively. We checked that there was no bias in the timing of concentration data: OSUR database has fixed and regular sampling frequencies while we noticed a few time series where summer periods were less sampled in the HYDRE/BEA data
125 for some years only.

Each C station was paired with a hydrometric station (Q). Observed daily streamflow data from the national hydrometric network (<http://hydro.eaufrance.fr/>) were used when draining headwater catchments for C and Q stations shared at least 80% of their areas (25% of cases). When observed Q data were not available, or at a frequency less than 320 measurements per year from 2007-2016 (75% of cases), discharge data were simulated using the GR4J model (Perrin et al., 2003). The headwater
130 catchments selected and their associated C and Q stations were distributed throughout Brittany (Fig. 1).

The 185 headwater catchments selected cover ca. 32% of Brittany's area. Despite having a similar hydrographic context dominated by subsurface flow, the catchments have large differences in topography, geology, hydrology, and diffuse and point-source pressures of N and P. We used a set of catchment descriptors to quantify this variability (Table-1) (see Supplemental S2 for their statistical distribution and S3 for their correlations). The descriptors selected included a set of spatial metrics for element sources (e.g. land use, pressure, soil contents) and for mobilization and retention processes (e.g. hydrology, climate, topography, geology, and soil properties).

The headwater catchments range in area from 5-179 km² (median of 38 km²), and the density of each one's hydrographic network ranges from 0.47-1.49 km.km⁻² (median of 0.90 km.km⁻²). Strahler stream order is 3 for 36% of the catchments, 2 for 18%, 4 for 17%, and 1 for 11%. Substrate composition is dominated by schists/micaschists (44%) or granites/gneisses (31%). In the topsoil horizon (0-30 cm), the soil organic C content varies greatly from 18.6-565.4 g.kg⁻¹ (median of 126.9 g.kg⁻¹), while the total P (Dyer method) content varies from 0.6-1.4 g.kg⁻¹ (median of 0.9 g.kg⁻¹). Land use is largely agricultural, although some catchments have high percentages of forested and urbanized areas. Riparian wetlands cover 12.3-36.3% of catchment area (median of 22.4%), forest covers 1.3-55.7% (median of 13.2%), pasture covers 10.3-46.7% (median of 25.6%), summer crops cover 6.5-50.3% (median of 27.8%), and winter crops cover 7.0-51.0% (median of 22.7%). The N and P surplus (potential diffuse agricultural sources) vary from 12.9-96.0 kg N.ha⁻¹.yr⁻¹ (median of 47.7) and 2.8-63.2 kg P.ha⁻¹.yr⁻¹ (median of 18.9), respectively. Urban areas cover 1.3-31.8% of the headwater catchments (median of 6%), with point-source input estimates ranging from 0-6.2 kg N. ha⁻¹.yr⁻¹ and 0-0.626 kg P. ha⁻¹.yr⁻¹. These data illustrate relative diversity in human pressures among the catchments despite a regional context of intensive agriculture. The daily mean flow (Q_{mean}) varies from 4.8-24.5 l.s⁻¹.km² (median of 10.8 l.s⁻¹.km²), the median of annual minimum of monthly flows (QMNA) varies from 0.2-5.9 l.s⁻¹.km², and the flow flashiness index (W2), defined as the percentage of total discharge that occurs during the highest 2% of flows (Moatar et al., 2020), ranges from 10-28%.

2.3 Data analysis

2.3.1 Concentration and load metrics

To analyze spatial variability in DOC, NO₃, and SRP concentrations in streams, we calculated their 10th, 50th, and 90th percentiles of concentration (C₁₀, C₅₀, and C₉₀, respectively) for each headwater catchment from 2007-2016. We also calculated the ratio of the coefficient of variation (CV) of mean concentration (CV_{C_{mean}}) and to that of mean flow (CV_{Q_{mean}}) to compare spatial variabilities in concentrations and stream flow. We estimated interannual loads for a 10-year period (2007-2016), with 8-12 C-Q values per year. However, a 5-year period (2010-2014) was considered to analyze the spatial variability because it minimized data gaps (in C and Q time series) among all stations simultaneously.

To calculate interannual DOC, NO₃, and SRP loads for each headwater catchment, we tested different methods and selected the most suitable, depending on the reactivity of the element with flow. When C-Q relationships were relatively flat or diluted

(NO₃) or slowly mobilized (DOC) during high flow (Q>Q₅₀), we used the discharge weighted concentration (DWC) method (Eq. 1), which estimates loads with lower uncertainties (Moatar and Meybeck, 2007; Raymond et al., 2013):

$$165 \quad \text{DWC} = \frac{k}{A} \times \frac{\sum_{i=1}^n C_i Q_i}{\sum_{i=1}^n Q_i} \bar{Q} \quad (1)$$

where DWC is the mean of annual loads (kg.y⁻¹.ha⁻¹), C_i is the instantaneous concentration (mg.l⁻¹), Q_i is the corresponding flow rate (m³.s⁻¹), \bar{Q} is the mean annual flow rate calculated from daily data (m³.s⁻¹), A is the area of the headwater catchment (km²ha), k is a conversion factor (31557.631536), and n is the number of C-Q pairs per year.

170 The loads estimated by the DWC method were corrected for bias (Moatar et al., 2013). Precisions were calculated from the number of samples (n), number of years, export regime exponent (b_{50high}), and W2 (Moatar et al., 2020).

To calculate SRP loads, regression methods were more suitable (because of strong concentration patterns when stream flow increases). We averaged the loads estimated by two regression methods developed by Raymond et al. (2013) – Integral Regression Curve (IRC) and Segmented Regression Curve (SRC) – both based on a regression between concentration and

175 flow:

$$\text{IRC} = \frac{k'}{A} \times \sum_{i=1}^n C_i Q_i \quad (2)$$

$$\text{SRC} = \frac{k'}{A} \times \left(\sum_{i=1}^{m1} C_{\text{infi}} Q_i + \sum_{i=1}^{m2} C_{\text{supi}} Q_i \right) \quad (3)$$

180 where IRC and SRC are the mean of annual loads (kg.y⁻¹.ha⁻¹); C_i, C_{supi}, and C_{infi} are instantaneous concentrations estimated by the regression curves (mg.l⁻¹); C_{supi} and C_{infi} are concentrations estimated for flows above and below the median flow, respectively; n = 365 days; m1 and m2 are numbers of days with daily flows below and above the median flow, respectively; and k' is a conversion factor (86.4). A is the area of the headwater catchment (ha).

2.3.2 Seasonal signal

185 Seasonal dynamics of discharge and solute concentrations were modeled using GAMs (Wood, 2017), which can estimate smoothed seasonal dynamics from time series (Musolff et al., 2017). The smoothing function was a cyclic cubic spline fitted to the month of the year (1-12); thus, the ends of the spline were forced to be equal, using the R package mgcv. We did not consider a long-term trend in the time series over the 10 years, for two reasons. First, significant long-term trends (according to Man-Kendall tests) had low slopes: mean Theil-Sen slopes ranged from -3% to 0% of the median concentration (while mean

190 seasonal relative amplitudes exceeded 50%). Second, performance of the GAMs did not increase significantly when a long-term trend was added: the mean adjusted coefficient of determination (Rsq) increased from 0.16 to 0.18 for DOC and from 0.30 to 0.40 for NO₃. We considered a seasonal dynamic to exist when the GAM adjusted coefficient of determination was

greater than 0.10. This method provides SI metrics on seasonality, which can be easily be linked to different geographical variables. However, it cannot take into account catchments without seasonality.

195 Seasonal dynamics of the concentrations of the three solutes (DOC, NO₃, and SRP) and river discharge were then analyzed using five metrics calculated from the daily simulations of the GAMs. The first three were the annual amplitude (Ampli; i.e. annual maximum minus annual minimum), and the mean time in which annual maximum and minimum concentrations occurred (MaxPhase and MinPhase, respectively; in months from 1 January). The next was Ampli standardized by the corresponding mean concentration to compare the three solutes. The last metric was a seasonality index (SI), which measures
200 the relative importance of summer (1 June to 31 July) concentrations compared to winter (15 January to 15 March) concentrations of an element, as follows (Eq. 4):

$$SI = \frac{C_{winter} - C_{summer}}{C_{winter} + C_{summer}} \quad (4)$$

where C_{winter} and C_{summer} are the averages of winter and summer concentrations, calculated from daily values from fitted
205 GAM. Positive values of SI (near 1) indicate that $C_{winter} > C_{summer}$, while negative values (near -1) indicate that $C_{winter} < C_{summer}$. We considered that SI values close to 0 (from -0.1 to 0.1) indicated that C_{winter} equaled C_{summer} . The SI integrates both amplitude and phasing features of the seasonal signal.

2.3.2 Statistical analyses

210 To compare the concentration metrics of the elements, a multivariate analytical approach, principal component analysis (PCA), was performed for the 9 variables of concentration percentiles (C10, C50, and C90) of DOC, NO₃, and SRP for the dataset of 185 headwater catchments. PCA was chosen despite it assumes linear relationships between variables, because it provides a graphical representation of correlations between variables or groups of variables and their contributions to the variance. To identify dominant drivers of spatial variability in concentration percentiles, seasonality, and loads of DOC, NO₃, and SRP, we
215 calculated Spearman's rank correlation (r_s) between these water-quality metrics and the descriptors of the headwater catchments. We considered a rank correlation to be significant if the corresponding p-value was ≤ 0.05 . All analyses were performed using R software (v. 3.6.1) with packages mgcv, hydroGOF, hydrostats, FactoMineR, tidyverse, lubridate, reshape2, plyr, ggcorrplot, and ggplot2 (Grolemund and Wickham, 2011; Le et al., 2008; Wickham, 2016, 2011; Wood, 2017; Zambrano-Bigiarini, 2020).

220

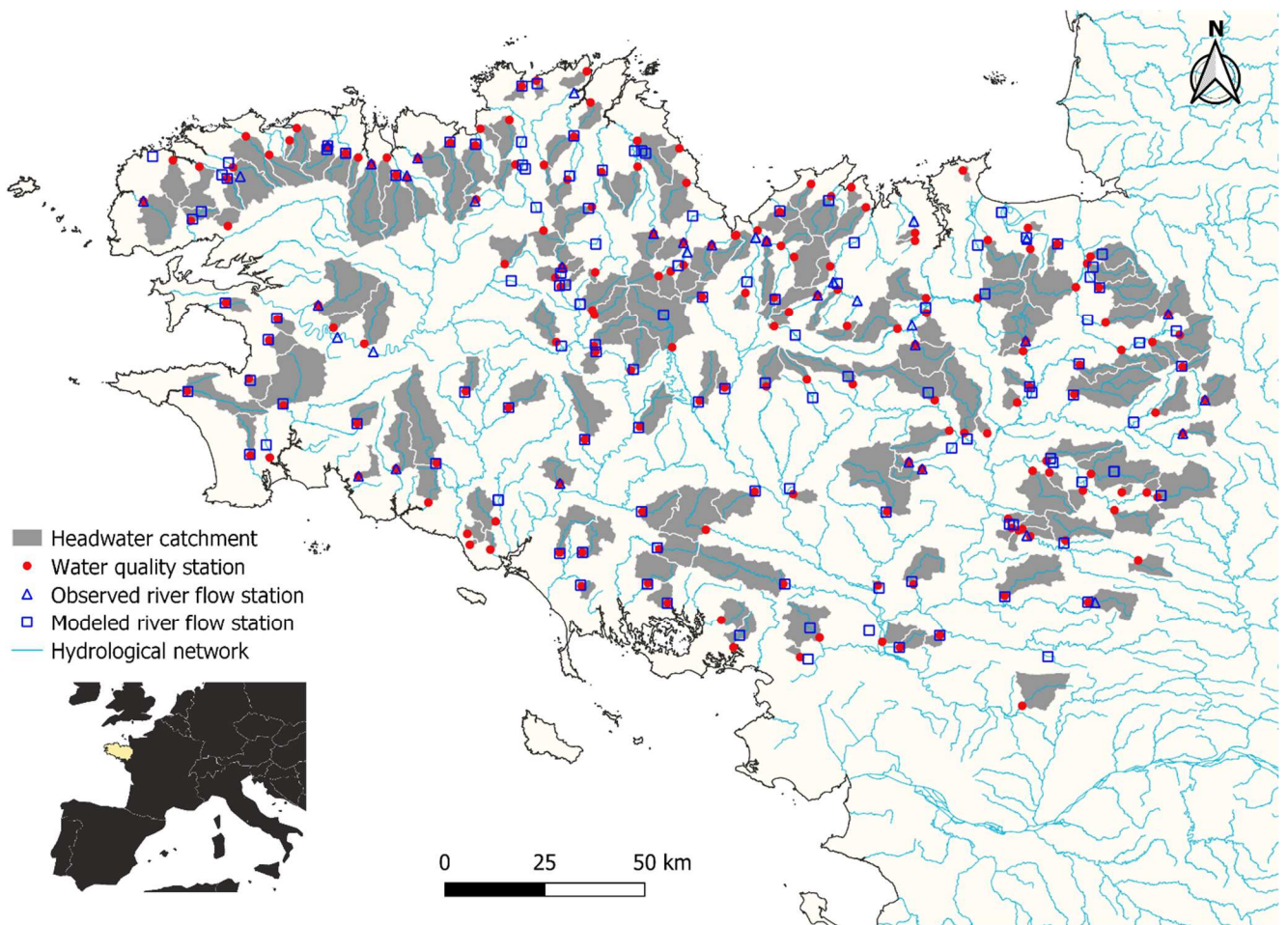


Figure 1. Locations of the 185 study headwater catchments where dissolved organic carbon, nitrate, and soluble reactive phosphorus concentrations were monitored monthly at the outlet from 2007-2016, and paired discharge stations where daily records of stream flow were available from observations or modeling.

Table 1. Headwater catchment descriptors identified as potential explanatory variables of spatial variability and temporal variation in dissolved organic carbon (DOC), nitrate (NO₃), and soluble reactive phosphorus (SRP) in stream and river water. $Topo_i = \log \frac{\alpha}{\tan \beta}$, (Beven and Kirkby, 1979), where α is the drainage area (ha) and β is the downstream slope (%), (Merot et al., 2003).^a there are 3 classes of soil thickness: 40-60 cm, 60-80 cm, 80-100 cm and >100 cm. ^b Winter crops have a winter plant cover and a phenological maximum in April (wheat, barley, rapeseed). ^c Summer crops correspond to bare winter soils and a phenological maximum in early summer (corn).

Type	Descriptor name	Unit	Definition	Source
Topography	Area	km ²	Drainage area of the monitoring station	Web-Processing Service "Service de Traitement de Modèles Numériques de Terrain" and DEM 50 m by IGN
	Elevation	m	Mean elevation of headwater catchment	DEM 25 m by IGN
	Density_hn	km.km ⁻²	Density of the hydrographic network	BD Carthage by IGN
	Topo_i	log(m ³)	Downstream topographic index of the headwater	BD Carthage by IGN
	IDPR	-	Hydrographic Network Development and Persistence Index	http://infoterre.brgm.fr/ BRGM data and geoservices portal (Mardhel and Gravier, 2004)
Geology	Granite_pm	%	Percentage of granite and gneiss area	Web-Mapping Service "Carte des Sols de Bretagne" by UMR 1069 SAS
	Schist_pm	%	Percentage of schist and micaschist area	INRAE – Agrocampus Ouest
	Other_pm	%	Percentage of various geological substrata	http://www.sols-de-bretagne.fr/
Soil	Erosion	%	Percentage of area with high to very high erosion risk (derived from land use, topography and soil properties)	Erosion risk map estimated from MESALES by GIS Sol, INRAE from Colmar et al. (2010)
	OC_soil	g.kg ⁻¹	Organic carbon content in the topsoil horizon (0-30 cm)	Web-Mapping Service from BDAT database, Saby et al. (2015) by GIS Sol
	Thick_soil	cm	Classes of dominant soil thickness ^a	Web-Mapping Service "Carte des Sols de Bretagne" by UMR 1069 SAS INRAE – Agrocampus Ouest
	TP_soil	g.kg ⁻¹	Total phosphorus content in the topsoil horizon (0-30 cm)	Web-Mapping Service from BDAT database by GIS Sol
Land-use	SummerCrop	%	Percentage of summer crop ^b land	
	WinterCrop	%	Percentage of winter crop ^c land	OSO database, CESBIO, land cover map 2016 (1 ha) from http://osr-eesbio.ups-tlse.fr/~oso/
	Forest	%	Percentage of forest land	
	Pasture	%	Percentage of pasture land	
	Urban	%	Percentage of urban land	
	Wetland	%	Percentage of potential wetlands	Web-Mapping Service "Enveloppe des milieux potentiellement humides de France réalisée par les laboratoires Infosol et UMR SAS" by UMR 1069

Diffuse and point N and P sources	N_surplus	kg.ha ⁻¹ .yr ⁻¹	Nitrogen surplus (= the maximum quantity on a given agricultural area that is likely to be transferred to the stream network)	CASSIS-N estimates by (Poisvert et al., 2017) from
	P_surplus	kg.ha ⁻¹ .yr ⁻¹	Phosphorous surplus	NOPOLU estimates by (Soes, 2013)
	N_point	kg.ha ⁻¹ .yr ⁻¹	Sum of nitrogen loads from domestic and industrial point sources	Data from Loire-Bretagne Water Agency data (2008-2012)
	P_point	kg.ha ⁻¹ .yr ⁻¹	Sum of phosphorus loads from domestic and industrial point sources	Data from Loire-Bretagne Water Agency (2008-2012)
Hydrology	Qmean	l.s ⁻¹ .km ⁻²	Interannual mean flow	
	QMNA	l.s ⁻¹ .km ⁻²	Median of annual minimum monthly specific discharge	Calculated from flow data observations: HYDRO regional database by DREAL Bretagne & GR4J simulations (Perrin et al., 2003)
	BFI	%	Base flow index (Lyne et Hollick, 1979)	
	W2	%	Percentage of total discharge that occurs during the highest 2% of flows (Moatar et al., 2013)	
	Rainfall	mm.yr ⁻¹	Mean effective rainfall from 2008-2012	SAFRAN database (8 km ²) by Météo France

Table 1. Headwater catchment descriptors identified as potential explanatory variables of spatial variability and temporal variation in dissolved organic carbon (DOC), nitrate (NO₃), and soluble reactive phosphorus (SRP) in stream and river water. $meanTWI = \log \frac{\alpha}{\tan \beta}$ (even and Kirkby, 1979), where α is the drainage area (ha) and β is the downstream slope (%). (Merot et al., 2003). ^a there are 3 classes of soil thickness: 40-60 cm, 60-80 cm, 80-100 cm and >100 cm. ^b Winter crops have a winter plant cover and a phenological maximum in April (wheat, barley, rapeseed). ^c Summer crops correspond to bare winter soils and a phenological maximum in early summer (corn).

Type	Descriptor name	Unit	Definition	Source
Topography	Area	km ²	Drainage area of the monitoring station	Web Processing Service “Service de Traitement de Modèles Numériques de Terrain” and DEM 50 m by IGN
	Elevation	m	Mean elevation of headwater catchment	DEM 25 m by IGN
	Density_hn	km.km ⁻²	Density of the hydrographic network	BD Carthage by IGN
	meanTWI	log(Ha)	Average topographic wetness index of the headwater catchment	DEM 25 m by IGN
	IDPR	=	Hydrographic Network Development and Persistence Index	http://infoterre.brgm.fr/ BRGM data and geoservices portal (Mardhel and Gravier, 2004)
Geology	Granite_pm	%	Percentage of granite and gneiss area	Web Mapping Service “Carte des Sols de Bretagne” by UMR 1069 SAS INRAE - Agrocampus Ouest http://www.sols-de-bretagne.fr/
	Schist_pm	%	Percentage of schist and micaschist area	
	Other_pm	%	Percentage of various geological substrata	
Soil	Erosion	%	Percentage of area with high to very high erosion risk (derived from land use, topography and soil properties)	Erosion risk map estimated from MESALES by GIS Sol, INRAE from Colmar et al. (2010)
	OC_soil	g.kg ⁻¹	Organic carbon content in the topsoil horizon (0-30 cm)	Web Mapping Service from BDAT database, Saby et al. (2015) by GIS Sol

	Thick soil	cm	Classes of dominant soil thickness ^a	Web Mapping Service “Carte des Sols de Bretagne” by UMR 1069 SAS INRAE - Agrocampus Ouest
	TP soil	g.kg ⁻¹	Total phosphorus content in the topsoil horizon (0-30 cm)	Web Mapping Service from BDAT database by GIS Sol
Land use	SummerCrop	%	Percentage of summer crop ^b land	OSO database, CESBIO, land-cover map 2016 (1 ha) from http://osr-cesbio.ups-tlse.fr/~oso/
	WinterCrop	%	Percentage of winter crop ^c land	
	Forest	%	Percentage of forest land	
	Pasture	%	Percentage of pasture land	
	Urban	%	Percentage of urban land	
	Wetland	%	Percentage of potential wetlands	Web Mapping Service “Enveloppe des milieux potentiellement humides de France réalisée par les laboratoires Infosol et UMR SAS” by UMR 1069 SAS INRAE - Agrocampus Ouest / US 1106 InfoSol INRAE
Diffuse and point N and P sources	N surplus	kg.ha ⁻¹ .yr ⁻¹	Nitrogen surplus (= the maximum quantity on a given agricultural area that is likely to be transferred to the stream network)	CASSIS-N estimates by (Poisvert et al., 2017) from https://geosciences.univ-tours.fr/cassis/login
	P surplus	kg.ha ⁻¹ .yr ⁻¹	Phosphorous surplus	NOPOLU estimates by (SoeS, 2013)
	N point	kg.ha ⁻¹ .yr ⁻¹	Sum of nitrogen loads from domestic and industrial point sources	Data from Loire-Bretagne Water Agency data (2008-2012)
	P point	kg.ha ⁻¹ .yr ⁻¹	Sum of phosphorus loads from domestic and industrial point sources	Data from Loire-Bretagne Water Agency (2008-2012)
Hydrology	Qmean	l.s ⁻¹ .km ²	Interannual mean flow	Calculated from flow data observations: HYDRO regional database by DREAL Bretagne & GR4J simulations (Perrin et al., 2003)
	QMNA	l.s ⁻¹ .km ²	Median of annual minimum monthly specific discharge	
	BFI	%	Base flow index (Lyne et Hollick, 1979)	
	W2	%	Percentage of total discharge that occurs during the highest 2% of flows (Moatar et al., 2013)	
	Rainfall	mm.yr ⁻¹	Mean effective rainfall from 2008-2012	

240 3 Results

3.1 Spatial variability in concentrations and loads

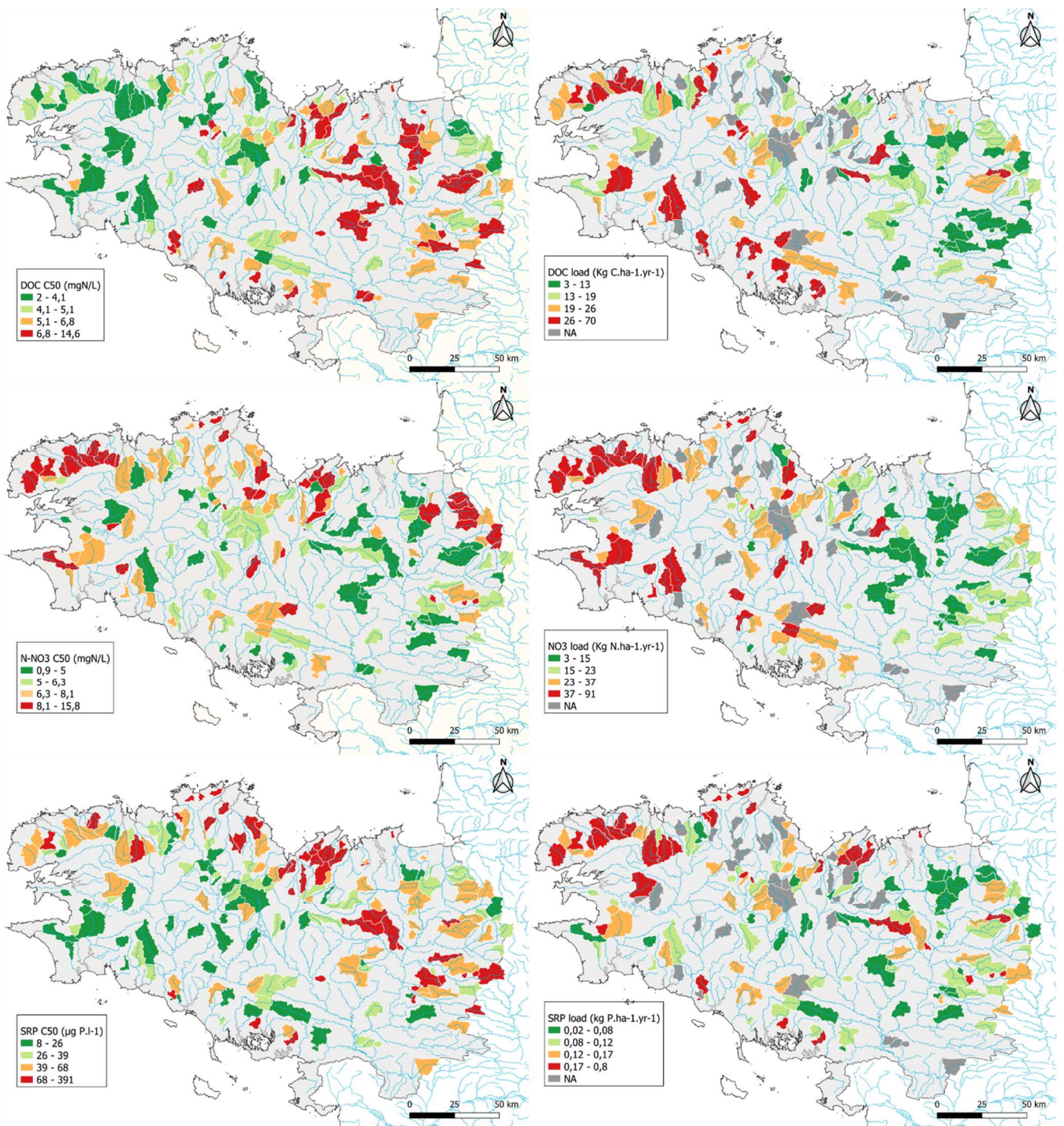
The C50 of the 185 headwater catchments ranged from 2-14.6 mg C.l⁻¹ for DOC, 0.9-15.8 mg N.l⁻¹ for NO₃, and 8-241 µg P.l⁻¹ for SRP (with 75% of the SRP C50 < 64 µg P.l⁻¹). The C50 displayed spatial gradients: rivers with DOC concentrations > 5 mg C.l⁻¹ were located in eastern Brittany, while the highest NO₃ concentrations were located on the west coast (Fig. 2). In contrast, the highest concentrations of SRP (C50 > 68 µg P.l⁻¹) were located in northern Brittany.

The two first axes of the PCA (Fig. 23a Supplemental S4a) performed on the percentiles of DOC, NO₃, and SRP concentrations of the 185 headwater catchments explained 58% of the variance and revealed three important points. First, percentiles (C10, C50, or C90) were grouped by solute, showing that the spatial organization remained the same regardless of the concentration percentile (Spearman rank correlations between the three indices always greater than 0.56 for all elements). Second, there was a negative correlation between the C50 of DOC and NO₃ concentrations (r_s = -0.58; Fig. 3b and Supplemental S3, S82 Supplemental S4b). Third, SRP concentrations had an orthogonal relation compared to DOC and NO₃ concentrations (r_s close to zero).

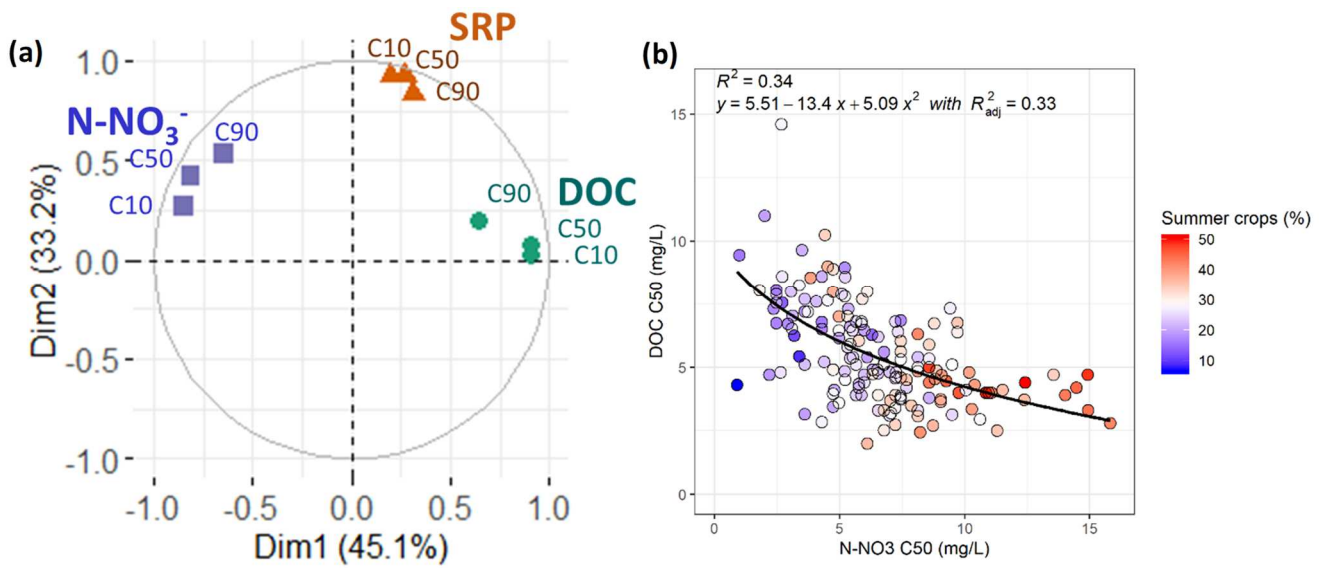
The ratios of mean concentration ($CV_{c_{mean}}$) to mean flow ($CV_{q_{mean}}$) were < 1 for DOC and NO_3 (Table 2), indicating that concentrations varied less in space than in flow, and vice-versa for SRP.

255 For DOC and NO_3 , Ampli was not correlated significantly with C50, but it was with C90 (Fig. 4 and Supplemental S83). For SRP, correlations between Ampli and the percentiles were high, with $r_s > 0.85$ for C50 and C90 (Fig. 34, Supplemental S8). The SI and phases, calculated on the catchments for which a GAM can be fitted, i.e. presenting a seasonal feature, were correlated more with C10 for DOC (n=107) and NO_3 (n=98) (negatively for SI and positively for the phases), and more with C90 for SRP (n=118) (negatively, for SI only).

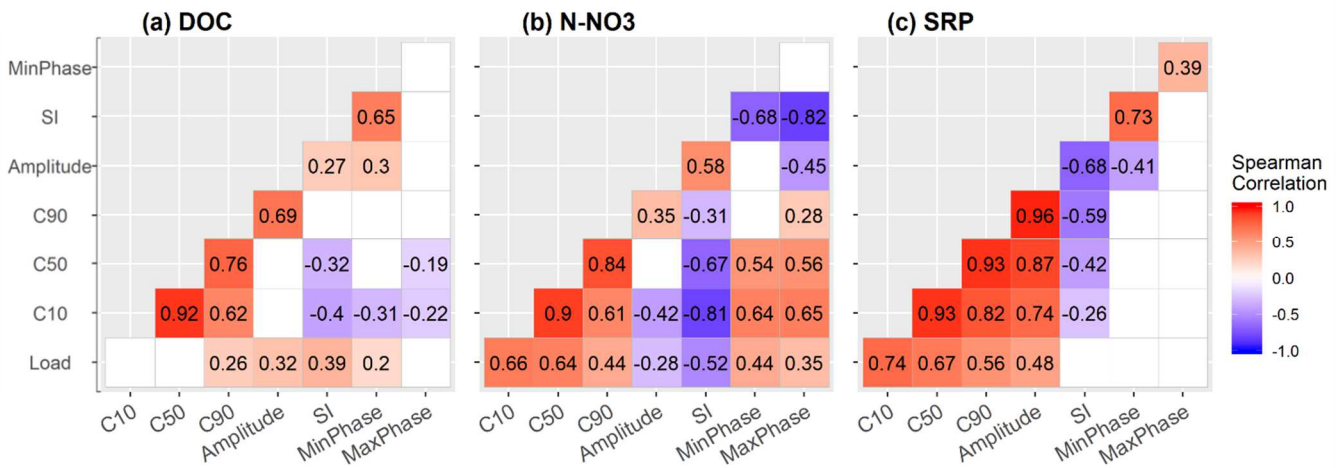
260 Mean (± 1 SD) interannual loads had high spatial variabilities – 20.71 ± 10.52 kg C.ha⁻¹.yr⁻¹ for DOC, 27.48 ± 18.51 kg N.ha⁻¹.yr⁻¹ for NO_3 , and 0.315 ± 0.11 kg P.ha⁻¹.yr⁻¹ for SRP – which differed from those observed for concentrations (Fig. 2). Unsurprisingly, interannual loads of the three solutes were significantly ($p < 0.001$) and strongly correlated with annual water fluxes (Pearson $r = 0.88$ for DOC, 0.90 for NO_3 , and 0.75 for SRP). There were weak but significant positive correlations between mean interannual loads and seasonality indices (Ampli, SI) or C90 for DOC (Fig. 34). Mean interannual loads of NO_3
265 were significantly and positively correlated with C10 and C50, and negatively with its seasonality indices. The strongest significant correlation was found between mean interannual loads and concentration percentiles for SRP.



270 **Figure 2.** Map of median (left) concentrations C50 and (right) loads of dissolved organic carbon (DOC), nitrate N (N-NO₃), and soluble reactive phosphorus (SRP) for the 185 streams. The catchments in gray did not meet the criteria to estimate a mean average interannual load. Classes in the legends have equal numbers of catchments.



275 **Figure 3.** (a) Principal component analysis of 10th, 50th, and 90th percentiles (C10, C50 and C90) of nitrate (N-NO₃⁻), dissolved organic carbon (DOC), and soluble reactive phosphorus (SRP) concentrations for the 185 headwater catchments analyzed; (b) Correlation between the medians (C50) of DOC and N-NO₃ concentrations for the 159 catchments in which DOC and NO₃ were monitored from 2007-2017. The color gradient indicates the percentage of catchment area covered by summer crops.



280 **Figure 4.** Matrices of Spearman's rank correlations of water quality (load, concentration percentiles (10th (C10), 50th (C50), and 90th (C90)), and seasonality metrics) for (a) dissolved organic carbon (DOC), (b) nitrate N (N-NO₃), and (c) soluble reactive phosphorus (SRP) (c). Only significant ($p \leq 0.05$) values are shown.

285

Table 2. Coefficients of variation (spatial variability among catchments) of flow-weighted mean concentration (CV_{cmean}) and mean stream flow (CV_{qmean}), and the value of their ratio, for dissolved organic carbon (DOC), nitrate (NO₃), and soluble reactive phosphorus (SRP).

Parameter	CV _{cmean}	CV _{qmean}	CV _{cmean} :CV _{qmean}
DOC	0.2954	0.4614	0.6403
NO ₃	0.3285	0.4709	0.6976
SRP	0.9207	0.4743	1.9412

290 3.2 Characterization of concentrations seasonality

3.2.1 Performance of GAMS

Of the 185 catchments, GAMS were fitted for 159 to DOC concentrations time series, 168 to NO₃ concentrations time series, 162 to SRP concentrations time series, and 185 to discharge time series. The cases for which fitting was not possible corresponded to those with no seasonal cyclicality or with excessive interannual variability. The percentage of variance explained by the GAM varied by site and solute. Fitting performed best for NO₃, followed by SRP and then DOC: the means and SDs of the adjusted Rsq were 0.30 ± 0.18 , 0.16 ± 0.11 , and 0.22 ± 0.15 for NO₃, DOC, and SRP, respectively (Supplemental S45 and S65), and the percentages of catchment for which the fitted model had Rsq > 0.20 were 67%, 52% and 38%, respectively. Metrics calculated from monthly data differed only moderately from those calculated from sub-monthly data (Supplemental S76), which tended to validate the approach of using monthly data.

300

3.2.2 Types of seasonal cyclicality in DOC, NO₃, and SRP

Most of the catchments had a seasonal concentration cycle: 85%, 71%, 78%, for NO₃, DOC, SRP concentration respectively and 100% of them had a seasonal discharge cycle (Fig. 54). Means and SDs of the standardized Ampli were 0.59 ± 0.46 for NO₃, 0.53 ± 0.30 for DOC, 0.79 ± 0.14 for SRP, and 1.99 ± 0.38 for discharge. The distribution of the calculated seasonality indices is provided in Supplemental S78.

305

The annual phases for discharge were more stable among all catchments than those for concentrations. The highest discharge period was centered on mid-February (winter) and the lowest discharge period on September. A strong gradient of hydrological dynamics was observed among catchments (Fig. 54d and Supplemental S78). The highest W2 was associated with both severe low-flow discharge and many high discharge events. Values of Q_{mean}, BFI, W2, and QMNA clearly followed an east-west gradient (not shown). Because of similar seasonal discharge dynamics in all catchments, SI can be used to describe the seasonal dynamics of a concentration relative to those of discharge. When SI was positive, the concentration seasonality was in-phase with discharge; when negative, the concentration seasonality was out-of-phase with discharge (Fig. 54).

310

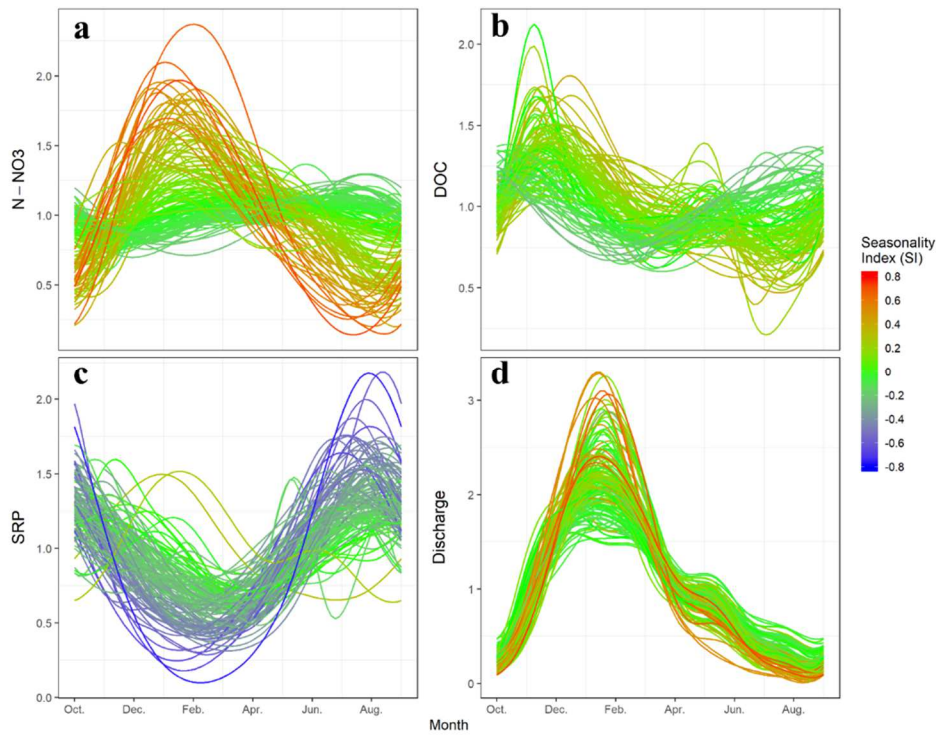
Most of the catchments had opposite dynamics for DOC and NO₃. For 90% of them, Pearson correlation between the daily GAM estimates of DOC and NO₃ was negative, and for 50% of the catchments, less than -0.79. The remaining 10% of catchments (15) had low Ampli of DOC and NO₃. The DOC and NO₃ concentrations had out-of-phase seasonal cycles, as shown by the negative correlation between SI and DOC or NO₃ for all catchments that had a significant seasonality in these concentrations (Fig. 65; R² = 0.62). We classified two types of catchments according to their seasonality in both DOC (MinPhase) and NO₃ (MaxPhase) concentrations and consistent with the SI (Fig. 65, Supplemental S78). NO₃ MaxPhase and DOC MinPhase that occurred before 1 May were classified as “in-phase” with discharge (Q), while those that occurred after were “out-of-phase” with Q, as proposed by (Van Meter et al. (2019)). All catchments experienced high stability of the DOC MaxPhase and NO₃ MinPhase were the same for all catchments as they always occurred between July and December (Fig. 54, Supplemental S87).

The first type, “in-phase” (68% of the catchments with seasonality), had a NO₃ MaxPhase between October and May (Fig. 45, Supplemental S78) (i.e. high-flow period, in-phase with maximum discharge and usually with DOC MinPhase). For these catchments, the mean SI was positive for NO₃ (0.22 ± 0.19) and usually negative or null for DOC (0.00 ± 0.13). They tended to be located toward central Brittany and be associated with mesoscale catchments (mean of 52.6 ± 38.8 km²). They had large Ampli for NO₃ and low Ampli for DOC (mean relative Ampli of 0.83 ± 0.46 , and 0.44 ± 0.23 for DOC) and relatively low C50 of NO₃ (means of 5.74 ± 2.46 mg N.l⁻¹ and 5.92 ± 2.00 mg C.l⁻¹).

The second type, “out-of-phase” (32% of the catchments with seasonality), had a DOC MinPhase and NO₃ MaxPhase between May and September (Fig. 45; Supplemental S87) (i.e. low-flow period, out-of-phase with maximum discharge). For most catchments, maximum NO₃ and minimum DOC concentrations occurred a mean of 1.85 months before minimum discharge or 5.5 months after maximum discharge, respectively. For these catchments, the mean SI was negative or null for NO₃ (-0.08 ± 0.06) and weakly positive for DOC (0.21 ± 0.10). These catchments were close to the coast and relatively small (mean of 31.4 ± 21.7 km²). They had smaller Ampli than “in-phase” catchments for NO₃, and higher Ampli for DOC (mean relative Ampli of 0.13 ± 0.13 , and 0.74 ± 0.30 for DOC) and relatively high C50 of NO₃ (means of 8.27 ± 2.90 mg N.l⁻¹ and 5.00 ± 1.62 mg C.l⁻¹).

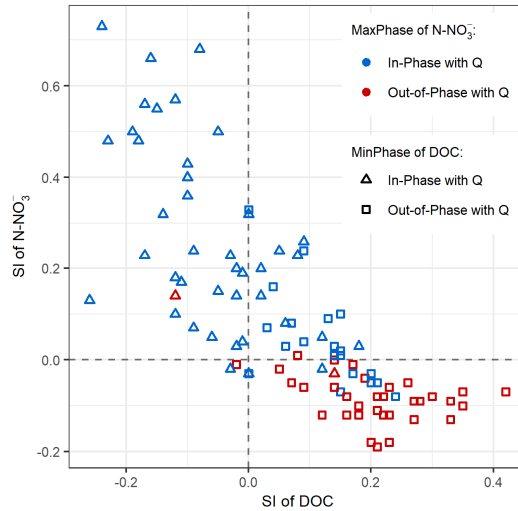
Some catchments had intermediate behavior between these two types (Figs. 45 and 56). Some had a plateau with maximum NO₃ and minimum DOC concentrations from winter to summer, while others showed two maxima for NO₃ or two minima for DOC (one synchronous with maximum discharge and another with minimum discharge). Other catchments also had maximum NO₃ synchronous with discharge, but minimum DOC after maximum discharge.

The seasonal dynamics of SRP were more stable than those of DOC and NO₃, but less stable than those of discharge. Thus, there was only one type of seasonality for SRP, which was out-of-phase with flow: MaxPhase SRP dominated in summer (mid-August ± 1.4 months), and MinPhase SRP dominated in late winter (March ± 1.2 months) (Fig. 54, Supplement S76), except for two catchments with maximum SRP in January-February.



350

Figure 54. Seasonal dynamics of: **a)** nitrate N ($N-NO_3$), **b)** dissolved organic carbon (DOC), **c)** soluble reactive phosphorus (SRP), and **d)** daily discharge modeled by Generalized Additive Models_s for 185 headwater catchments. To compare concentrations, they are standardized by their mean interannual concentration. The color gradient represents the seasonality index of each parameter; thus, a headwater catchment's color can vary among panels.



355

Figure 65. Relationship between the seasonality indices (SI) of nitrate N ($N-NO_3$) vs. dissolved organic carbon (DOC) in the headwater catchments for which seasonality was significant for both parameters ($n=98$). The color and shape of symbols identify the seasonality types based on the NO_3 MaxPhase and DOC MinPhase metrics. The threshold date was 1 May: MaxPhase that

occurred before were classified as “in-phase” with discharge (Q), while those that occurred after were “out-of-phase” with Q. The DOC MinPhase metric is shown to highlight the synchrony between minimum DOC and maximum N-NO₃ concentrations.

3.3 Controlling factors of concentration and discharge percentiles and seasonality

360 The C50 of DOC was correlated significantly with 15 spatial variables and most strongly ($|r_s| \geq 0.4$) with topographic index, QMNA, and the other hydrological indices. The C50 of NO₃ was correlated significantly with 12 spatial variables, in particular diffuse agricultural sources ($r_s = -0.68$ for the percentage of summer crops, $r_s > 0.39$ for N and P surplus, and $r_s = -0.48$ for soil erosion rate) and hydrological indices, through the base flow index (BFI) (positively) and W2 (negatively), (Table 3). The C50 of SRP was correlated significantly with more variables (18), but the correlations were slightly weaker. It correlated most strongly with soil P stock ($r_s = -0.40$), climate and hydrology ($r_s = -0.43$ to -0.34 with effective rainfall, Qmean, QMNA), elevation, and hydrographic network density. It had weaker positive correlations ($r_s < 0.3$) with the soil erosion rate and domestic and agricultural pressures (urban percentage and P surplus).

Ampli and SI for DOC and NO₃ were correlated most with the hydrodynamic properties, followed by agricultural pressures (Fig. 76, Table 3). The catchments “in-phase” with discharge (i.e. positive SI-NO₃ and negative SI-DOC correlations) were associated with high hydrological reactivity (low BFI and high W2) and a low percentage of summer crops (Table 3). Conversely, catchments “out-of-phase” with discharge (i.e. negative SI-NO₃ and positive SI-DOC correlations) were associated with low hydrological reactivity (high BFI and QMNA, low W2) and a high percentage of summer crops.

370 Correlations of SI with catchment descriptors were weaker ($|r_s| \leq 0.4$) for SRP than for DOC, ~~and~~ NO₃ and discharge because most catchments had the same seasonal pattern, with maximum SRP concentration during low flow. Catchments with the highest amplitudes of SRP concentration were associated with low QMNA and Qmean, high W2, low effective rainfall, and low soil P stock. Interannual loads were correlated mainly with hydrological descriptors (positively with Qmean and QMNA, and negatively with W2) (Table 3). Interannual NO₃ loads were also correlated with the percentage of summer crops and soil TP content, while interannual SRP loads were correlated weakly with the percentage of summer crops, agricultural surplus, erosion, and point sources. Discharge indicators present some obvious correlations (e.g. Q50 and annual amplitude with Qmean and QMNA). Q50, and in a lower degree, annual amplitude are positively correlated with baseflow index (BFI), and negatively correlated with flow flashiness (W2). This indicates that in catchments where streams are more influenced by groundwater (generally those flowing on granite), BFI is high and flow flashiness is low.

385 Correlations with catchment characteristics are lower than expected for the Q50. Q50 is significantly correlated with wetness topographic index (meanTWI, $r_s = -0.53$) which indicates that Q50 is increasing in catchments with drier soils (meanTWI low). Positive correlation with granite indicates that discharge is more supported by this type of rocks, which present favorable groundwater storage. Q50 is positively correlated with soil TP, which is higher on granite substratum. Q50 is positively correlated with SummerCrop and negatively with WinterCrop, underlying higher runoff in catchments with non-cultivated soil during winter.

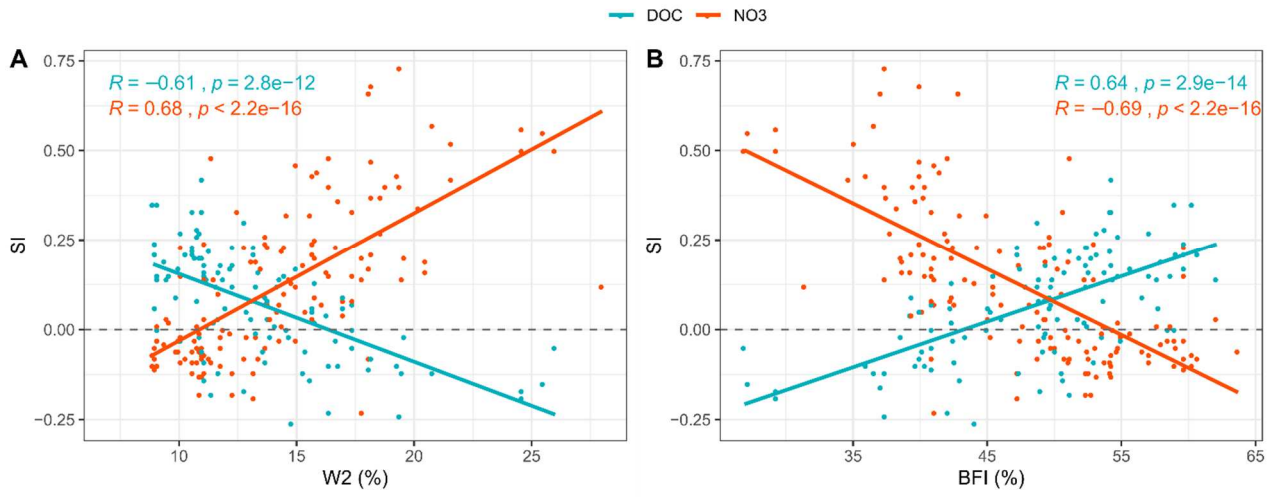


Figure 67. Relationship between the seasonality index (SI) of dissolved organic carbon (DOC) and nitrate (NO₃) and the hydrological reactivity descriptors (A) flow flashiness index (W2) and (B) base-flow index (BFI) for 124 headwater catchments.

Table 3. Spearman rank correlations between water quality indices and geographical descriptors for dissolved organic carbon (DOC), nitrate (NO₃), and soluble reactive phosphorus (SRP). Only significant correlations (p≤0.05) are shown, and bold text indicates |r|≥0.40.

Spatial variable	DOC				NO ₃				SRP			
	C50	Ampli	SI	Load	C50	Ampli	SI	Load	C50	Ampli	SI	Load
Topography	Area	-	-0.24	-	-	-	-	-	-	-	-	-
	Elevation	-0.46	-0.18	-	-	-	-0.31	-0.20	0.19	-0.20	-	-
	Density_hn	-	-	-	-	-	-0.22	-	0.16	-0.30	-0.27	0.19
	Topo_i	0.54	-	-	-	-	0.41	0.25	-0.33	0.39	0.25	-
	IDPR	-	-	-	-	-	-	-	-	-0.21	-0.19	-
Geology	Granite_pm	-	-	0.21	0.41	-	-0.43	-0.31	0.27	-0.26	-0.24	-
	Schist_pm	-	-0.21	-0.37	-0.29	-0.16	0.25	0.22	-0.23	-	-	-0.20
	Other_pm	-	0.32	0.35	-	0.28	-	-	-	0.28	0.16	-
Soil	Erosion	-0.36	0.24	-	-	0.48	0.16	-0.26	0.39	0.24	0.17	-
	OC_soil	-0.27	-0.21	-	-	-	-0.29	-	0.18	-0.20	-0.19	-
	TP_soil	-0.44	-	-	0.38	-	-0.51	-0.34	0.49	-0.40	-0.32	-
Land-use	SummerCrop	-0.30	0.28	0.54	-	0.68	-	-0.47	0.54	-	-	0.29
	WinterCrop	0.19	-	-0.20	-0.29	-	0.48	0.21	-0.23	0.17	-	-0.18
	Forest	-	-0.17	-0.30	0.23	-0.37	-0.47	-	-	-0.29	-0.19	-
	Pasture	-	-	-	-	-0.30	-	0.26	-0.20	-	-	-
	Urban	-	-	-	-	-	-	-	-	0.23	-	-
N and P diffuse and point sources	N_surplus	-0.21	0.20	-	-	0.39	-	-	0.38	-	-	0.29
	P_surplus	-0.24	0.33	-	-0.22	0.49	-	-0.32	0.37	0.20	-0.19	-
	N_point	-	-0.17	-	-	-	-	-	-	-	-	-
	P_point	-	-0.16	-	-	-	-	-	0.21	-	-	0.21
Hydrology	Qmean	-0.49	0.19	-	0.53	0.16	-0.58	-0.42	0.67	-0.39	-0.31	0.21
	QMNA	-0.52	0.25	0.41	0.48	0.42	-0.54	-0.56	0.76	-0.34	-0.32	0.35
	BFI	-0.41	-0.27	0.64	0.38	0.54	-0.52	-0.69	0.57	-0.20	-0.23	0.32
	W2	0.43	-	-0.61	-0.46	-0.49	0.54	0.68	-0.59	0.20	0.20	-0.26
	Precipitation	-0.50	-	-	0.47	-	-0.60	-0.39	0.60	-0.43	-0.33	0.18
	Wetland	0.16	-	0.31	0.38	-	-	-	-	-	-	0.35

405 Table 3. Spearman rank correlations between water quality indices for dissolved organic carbon (DOC), nitrate (NO₃), soluble reactive phosphorus (SRP), discharge indices (Q) and geographical descriptors. Only significant correlations (p≤0.05) are shown, and bold text indicates |r| ≥ 0.40.

Spatial variable	DOC				NO ₃				SRP				Q	
	C50	Ampli	SI	Load	C50	Ampli	SI	Load	C50	Ampli	SI	Load	Q50	Ampli
Topography														
Area	-	<u>-0.24</u>	-	-	-	-	-	-	-	-	-	-	-	-
Elevation	-0.46	<u>-0.18</u>	-	-	-	<u>-0.31</u>	<u>-0.20</u>	<u>0.19</u>	<u>-0.20</u>	-	-	<u>0.38</u>	<u>0.38</u>	<u>0.37</u>
Density_hn	-	-	-	-	-	<u>-0.22</u>	-	<u>0.16</u>	<u>-0.30</u>	<u>-0.27</u>	<u>0.19</u>	<u>0.25</u>	<u>0.25</u>	-
meanTWI	0.54	-	-	-	-	0.41	<u>0.25</u>	<u>-0.33</u>	<u>0.39</u>	<u>0.25</u>	-	-0.53	-0.53	-0.59
IDPR	-	-	-	-	-	-	-	-	<u>-0.21</u>	<u>-0.19</u>	-	<u>0.20</u>	<u>0.20</u>	-
Geology														
Granite_pm	-	-	<u>0.21</u>	0.41	-	-0.43	<u>-0.31</u>	<u>0.27</u>	<u>-0.26</u>	<u>-0.24</u>	-	0.43	0.43	<u>0.35</u>
Schist_pm	-	<u>-0.21</u>	<u>-0.37</u>	<u>-0.29</u>	<u>-0.16</u>	<u>0.25</u>	<u>0.22</u>	<u>-0.23</u>	-	-	-	<u>-0.25</u>	<u>-0.25</u>	-
Other_pm	-	<u>0.32</u>	<u>0.35</u>	-	<u>0.28</u>	-	-	-	<u>0.28</u>	<u>0.16</u>	-	-	-	-
Soil														
Erosion	<u>-0.36</u>	<u>0.24</u>	-	-	0.48	<u>0.16</u>	<u>-0.26</u>	<u>0.39</u>	<u>0.24</u>	<u>0.17</u>	-	-	-	-
OC_soil	<u>-0.27</u>	<u>-0.21</u>	-	-	-	<u>-0.29</u>	-	<u>0.18</u>	<u>-0.20</u>	<u>-0.19</u>	-	<u>0.34</u>	<u>0.34</u>	<u>0.32</u>
TP_soil	-0.44	-	-	<u>0.38</u>	-	-0.51	<u>-0.34</u>	0.49	-0.40	<u>-0.32</u>	-	0.78	0.78	0.71
Land use														
SummerCrop	<u>-0.30</u>	<u>0.28</u>	0.54	-	0.68	-	-0.47	0.54	-	-	<u>0.29</u>	<u>0.29</u>	<u>0.29</u>	-
WinterCrop	<u>0.19</u>	-	<u>-0.20</u>	<u>-0.29</u>	-	0.48	<u>0.21</u>	<u>-0.23</u>	<u>0.17</u>	-	<u>-0.18</u>	-0.51	-0.51	<u>-0.34</u>
Forest	-	<u>-0.17</u>	<u>-0.30</u>	<u>0.23</u>	<u>-0.37</u>	-0.47	-	-	<u>-0.29</u>	<u>-0.19</u>	-	-	-	<u>0.25</u>
Pasture	-	-	-	-	<u>-0.30</u>	-	<u>0.26</u>	<u>-0.20</u>	-	-	-	-	-	-
Urban	-	-	-	-	-	-	-	-	<u>0.23</u>	-	-	-	-	-
N and P diffuse and point sources														
N_surplus	<u>-0.21</u>	<u>0.20</u>	-	-	<u>0.39</u>	-	-	<u>0.38</u>	-	-	<u>0.29</u>	<u>0.28</u>	<u>0.28</u>	-
P_surplus	<u>-0.24</u>	<u>0.33</u>	-	<u>-0.22</u>	0.49	-	<u>-0.32</u>	<u>0.37</u>	<u>0.20</u>	<u>-0.19</u>	-	<u>0.20</u>	<u>0.20</u>	-
N_point	-	<u>-0.17</u>	-	-	-	-	-	-	-	-	-	-	-	-
P_point	-	<u>-0.16</u>	-	-	-	-	-	<u>0.21</u>	-	-	-	-	-	-
Hydrology														
Qmean	-0.49	<u>0.19</u>	-	0.53	<u>0.16</u>	-0.58	-0.42	0.67	<u>-0.39</u>	<u>-0.31</u>	<u>0.21</u>	0.95	0.95	0.90
QMNA	-0.52	<u>0.25</u>	0.41	0.48	0.42	-0.54	-0.56	0.76	<u>-0.34</u>	<u>-0.32</u>	<u>0.35</u>	0.94	0.94	0.70
BFI	-0.41	<u>-0.27</u>	0.64	<u>0.38</u>	0.54	-0.52	-0.69	0.57	<u>-0.20</u>	<u>-0.23</u>	<u>0.32</u>	0.72	0.72	<u>0.21</u>
W2	0.43	-	-0.61	-0.46	-0.49	0.54	0.68	-0.59	<u>0.20</u>	<u>0.20</u>	<u>-0.26</u>	-0.76	-0.76	<u>-0.30</u>
Precipitation	-0.50	-	-	0.47	-	-0.60	<u>-0.39</u>	0.60	-0.43	<u>-0.33</u>	<u>0.18</u>	0.88	0.88	0.86
Wetland	<u>0.16</u>	-	<u>0.31</u>	<u>0.38</u>	-	-	-	-	-	-	-	-	-	-

4 Discussion

4.1 Interpretation of the spatial opposition between DOC and NO₃

Spatial opposition between DOC and NO₃ concentrations has been reported for a wide range of ecosystems. Taylor and Townsend (2010) found a non-linear negative relationship between them for soils, groundwater, surface freshwater, and oceans, from global to local scales, and highlighted that this negative correlation prevails in disturbed ecosystems. Goodale et al. (2005) reported a similar negative correlation among 100 streams in the northeastern USA. Heppell et al. (2017) found that DOC and NO₃ concentrations were inversely correlated with the BFI in six reaches of the Hampshire Avon catchment (UK). Our contribution brings an original focus on this relationship in headwater catchments with high domestic and agricultural pressures. Taylor and Townsend (2010) interpreted this spatial opposition as a response of microbial processes (i.e. biomass production, nitrification, and denitrification) to the ratio of ambient DOC:NO₃, which controls NO₃ export/retention in catchments (see also Goodale et al. (2005)). In semi-natural ecosystems, high but poorly labile soil organic C pools were associated with lower N retention capacity and thus higher N leaching (Evans et al., 2006). Similarly, several studies (e.g. Hedin et al., 1998; Hill et al., 2000) suggested that DOC supply limits in- and near-stream denitrification. In contrast, other studies claimed that N can influence loss of DOC from soils by altering substrate availability or/and microbial processing of soil organic matter (Findlay, 2005; Pregitzer et al., 2004). In our study, C50 were correlated with both BFI and QMNA, positively for NO₃ and negatively for DOC, which suggests that catchments strongly sustained by groundwater flow produced higher NO₃ and lower DOC concentrations, as reported in other rural catchments (e.g. Heppell et al., 2017). The C50 of NO₃ increased with agricultural pressures (percentage of summer crop, N surplus), as observed by Lintern et al. (2018), while that of DOC increased in flatter catchments, which is consistent with results of Mengistu et al. (2014) and Musolff et al. (2018). This suggests that this spatial opposition between DOC and NO₃ results from the combination of heterogeneous human inputs, heterogeneous natural pools, and different physical and biogeochemical connections between C and N pools. In surface water, these heterogeneous sources are expressed to differing degrees depending on the catchment's hydrological behavior. When deep or slow flowpaths dominate, they store and release N via groundwater and mobilize little the sources rich in organic matter. When shallower and faster flowpaths dominate, they transport some of the N via compartments rich in organic matter, which causes N depletion and release of more DOC to the streams. The initial amounts of NO₃ along these flowpaths are a function of human pressures.

4.2 Interpretation of the temporal opposition between DOC and NO₃

The seasonal opposition between DOC and NO₃ concentration dynamics could be another manifestation of the spatial opposition between DOC and NO₃ sources, because the strength of the hydrological connection between sources and streams

varies seasonally (e.g. Mulholland and Hill (1997); Weigand et al. (2017)). The direct contribution of biogeochemical reactions that connect DOC and NO₃ cycles may also vary seasonally (Mulholland and Hill, 1997; Plont et al., 2020). Indeed, temperature, wetness condition, and light availability influence rates of these organic matter reactions (Davidson et al., 2006; Hénault and Germon, 2000; Luo and Zhou, 2006). In addition, the relative importance of the fluxes produced or consumed via these reactions appears clearer during the low-flow period, when the fluxes exported from the terrestrial ecosystem and delivered to the stream decrease. These reactions consume NO₃ (e.g. denitrification, biological uptake) and release (reductive dissolution) or produce (autotrophic production) DOC. Of the two seasonal NO₃-DOC cycles, the most common in our datasets is thus maximum NO₃ in-phase with maximum discharge and minimum DOC, which has been reported in Brittany (Abbott et al., 2018b; Dupas et al., 2018) and elsewhere (Van Meter et al., 2019; Dupas et al., 2017; Halliday et al., 2012; Minaudo et al., 2015; Weigand et al., 2017). The main control of seasonal DOC-NO₃ cycles appears to be related to hydrological indices (expressed as BFI and W2). Hydrological flashiness reflects the relative importance of subsurface flow compared to deep base flow (Heppell et al., 2017); thus, low BFI (or high W2) would indicate higher connectivity with subsurface riparian sources and shorter transit times. This is consistent with results of Weigand et al. (2017), who observed higher seasonal amplitudes in DOC and NO₃ concentrations and stronger temporal anti-correlation between DOC and NO₃ concentrations in stream water dominated by subsurface runoff.

Our results are consistent with these previous results, while the correlations with catchment characteristics can provide some explanation. Catchments with low BFI have larger shallow flows and experience seasonal DOC-NO₃ cycles that are in-phase with flow and have higher NO₃ amplitudes. These cycles can be interpreted as the combination of several mechanisms (Fig. 87):

- 1) Synchronization at the same time, of NO₃-rich and DOC-poor groundwater contribution with maximum flow.
- 2) Large contribution of near-/in-stream biogeochemical processes at reduced low flows that decreases NO₃ concentration (e.g. NO₃ consumption by aquatic microorganisms, biofilms, ~~and~~ macrophytes, and redox processes).
- 3) Large DOC-rich riparian contribution throughout the year, but larger in autumn, when flow starts to increase, as described in detail in previous AgrHys Observatory studies (Aubert et al., 2013; Humbert et al., 2015).

In contrast, catchments with higher BFI have smaller shallow flows and experience mainly DOC and NO₃ cycles that are out-of-phase with flow and have lower amplitudes. These cycles can be attributed to the following:

- 1) More continuous groundwater contribution, combined with a decrease in agricultural pressures over time, and consequently, a decrease NO3 concentration more in shallower and younger groundwater than in deeper, older groundwater ~~which could increase NO3 concentrations more in deeper groundwater than in shallower groundwater~~ (Abbott et al., 2018b; Martin et al., 2004; Martin et al., 2006). This vertical gradient in groundwater supply could explain why NO₃ concentrations peaked during the annual discharge recession, which is sustained mainly by deep groundwater inputs.
- 2) Little contribution of near-/in-stream biogeochemical processes at reduced low flows due to larger inputs from groundwater, which maintains a relatively high minimum NO₃ concentration.

- 3) Contribution of DOC-rich riparian sources, mainly in autumn, that are smaller than those in in-phase catchments, again due to a predominantly deeper geometry of water circulation.

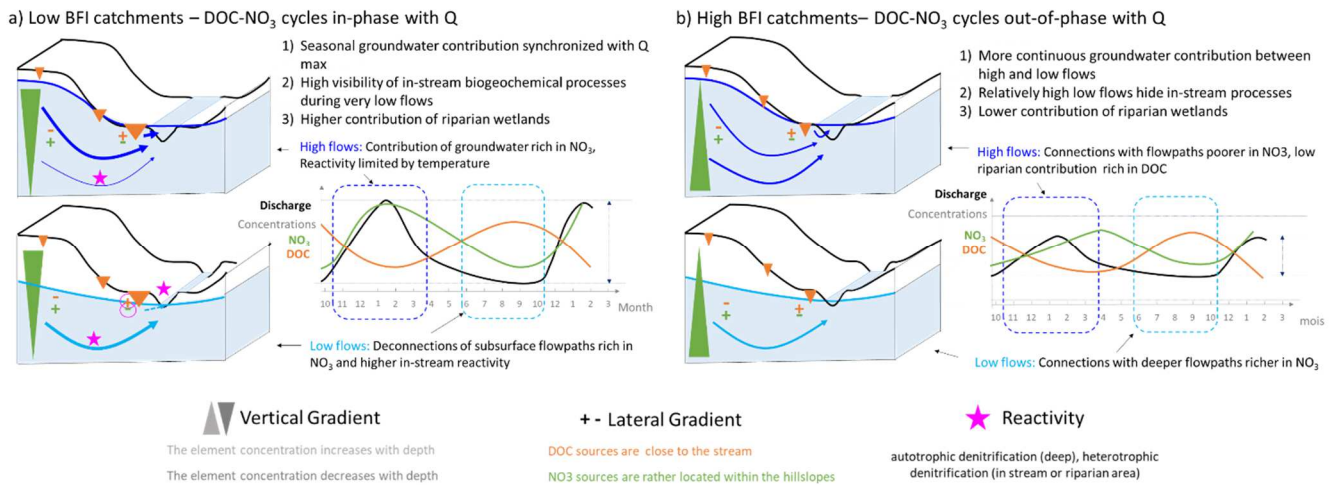


Figure 87. Conceptual diagram of seasonal flowpaths involved in the DOC-NO₃ seasonal cycles leading to a) in-phase cycles with discharge or b) out-of-phase cycles with discharge.

4.3 Interpretation of the spatial and temporal signature of SRP

The correlations between the C50 of SRP and geographic variables highlighted the importance of P sources (soil P stocks, followed by domestic and agricultural pressures) and surface flowpaths (e.g. hydrological indices, elevation, erosion risk). Similarly, analysis of regression models that predicted spatial variability in total P concentration of 102 rural catchments in Australia also indicated positive effects of human-modified land uses, natural land uses prone to soil erosion, mean P content of soils, and to a lesser extent, topography (Lintern et al., 2018). They always included the percentage of urban area, which suggests a considerable effect of sewage discharge, even at low levels of urbanization. The catchments analyzed in the present study have a homogeneous and relatively dense distribution of small villages but no large city, which seems to support this last hypothesis. Sobota et al. (2011) studied spatial relationships among P inputs, land cover and mean annual concentrations of different forms of P in 24 catchments in California, USA. They found that P concentrations were significantly correlated with agricultural inputs and, to a lesser extent, agricultural land cover but not with estimates of sewage discharge. Nonpoint sources of P in agricultural runoff, historical inputs of fertilizer and manure in excess of crop requirements have led to a build-up of soil P levels, particularly in areas of intensive crop and livestock production (Sharpley et al., 1994). This led to correlations between soil P and runoff concentrations in agricultural catchments (Cooper et al., 2015; Sandström et al., 2020), as found here.

The seasonality of SRP was generally the same in the region studied, and C50 and amplitudes were significantly correlated. A peak in seasonal SRP concentrations at low flow has been reported previously (Abbott et al., 2018b; Bowes et al., 2015; Dupas

et al., 2018; Melland et al., 2012). It is interpreted as the result of a dominance of point sources diluted during high flow (Minaudo et al., 2019, 2015; Bowes et al., 2011) or of stream-bed sediment sources for which P release increases with
500 temperature (Duan et al., 2012).

Correlation between spatial patterns of NO₃ and SRP was expected given the dominant agricultural origin of N and substantial agricultural origin of P, but it was not observed in all catchments. The C50 of NO₃ and SRP were high mainly on the northwestern coast, perhaps due to intensive vegetable production associated with a dominance of mineral fertilization (Lemercier et al., 2008). Elsewhere, a high proportion of allochthonous P in the topsoil results from livestock farming and
505 manure application (Delmas et al., 2015). The P-retention capacity of soils (related to their Al, Ca, Fe, and clay contents) is also likely to increase spatial variability in the release of P from catchments (Delmas et al., 2015). Synchronous variations in SRP and DOC, such as those observed in small, completely agricultural headwater catchments without villages (Cooper et al., 2015; Dupas et al., 2015b; Gu et al., 2017), were not observed in the present set of catchments. We assume that synchronicity of SRP and DOC in small catchments depends on soil processes, such as reduction of soil Fe-oxyhydroxides in wetland zones
510 (Gu et al., 2019), which are hidden by in-stream processes (P adsorption on streambed sediments) and downstream point-source inputs (especially P inputs) in the set of larger catchments studied.

Regarding the geographic data used as spatial descriptors, the region studied did not have a few dense urban centers but rather smaller domestic points scattered across the region, which is harder to characterize finely. Moreover, Brittany's coastlines may have higher population densities in spring and summer due to tourism. Refined estimates of domestic point sources and their
515 seasonal variations would be useful in future analyses.

4.4 Hydrological vs. anthropogenic controls of spatial variability in water quality

Among the headwater catchments selected, the human pressures (agriculture for NO₃ and sewage water discharge for SRP) influenced the C50 and loads of NO₃ and SRP. However, the influence of hydrological descriptors on the spatial variability in
520 their loads suggested a transport-limited behavior of these catchments (Basu et al., 2010). Nutrient load estimates had high uncertainties due to i) using modeled flow data when measurements were not available and ii) the frequency of concentration data (monthly), which is low for estimating nutrient loads (especially of P) (Raymond et al., 2013). Thus, these load estimates allowed only their relative spatial variation to be analyzed. Although land-use or agricultural pressure variables, in combination with rainfall and discharge variables, are good predictors of nutrient loads at larger scales (Dupas et al., 2015a; Grizzetti et al.,
525 2005; Preston et al., 2011), the correlations with loads were lower in the set of headwater catchments selected. For NO₃, this can be explained by higher spatial variability (CVs) in water fluxes than in concentrations (Table 2), which can explain the dominance of hydrological fluxes in the spatial organization of nutrient loads. Such dominance was found to increase with the level of human pressure in Thompson et al. (2011) for NO₃. In this study, such relationship was not visible as all the catchments exhibited a transport-limited behavior. It may also suggest that the nutrient-surplus data at the local scale remained uncertain

530 (Poisvert et al., 2017) or that at this scale, data on agricultural practices would be more relevant, and that variability in concentration depends less on the magnitude of nutrient inputs than on their locations.

The catchments studied have clear seasonal dynamics in concentration, which is consistent with previous observations (Minaudo et al., 2019; Abbott et al., 2018a). The seasonal pattern is controlled mainly by hydrological variables. It partly reflects the mixing of contrasting sources that are connected to streams by seasonally varying flowpaths with nutrients that are transferred vs. nutrients that are processed locally in hotspots (e.g. riparian buffer, stream water, stream sediments) or delivered over point sources. The seasonal NO₃-DOC pattern seemed to become somewhat homogenous among catchments larger than 100 km², where seasonal cycles with maximum NO₃ in-phase with flow seemed less common. This may be related to an increase in in-stream biological activity during summer as catchment size increases, enhanced by a lower stream water level and slower discharge (Minaudo et al., 2015). Therefore, the potential relationship between seasonal cycle type and catchment size should be studied over a wider range of catchment sizes and nested catchments to include variations along the hydrographic network.

4.5 Implications for headwater monitoring and management

The high regional and seasonal variations of nutrient concentrations in streams probably drive high variations of nutrient stoichiometry along the water-year hydrological cycle and over the region, and, consequently, high variations in time and space of eutrophication risks downstream (Westphal et al., 2020). Due to the combination of anthropogenic and hydrological drivers in explaining these stream concentrations, a better estimation on nutrient inputs and discharge in all headwater catchments is important to predict areas at risks, as a first step, ~~is important to predict areas at risks~~. The spatial analysis shows high and poorly structured spatial variations of concentrations over the region. Nevertheless, the opposition between NO₃ and DOC concentrations suggests that the C:N ratios will be even more variable:

- 1) In space: catchments with high DOC C50 and low NO₃ C50 will exhibit very high C:N and vice versa
- 2) Over the seasons: as minimum of DOC and maximum of NO₃ concentrations are in-phase: catchment where DOC-NO₃ variations are in phase with Q will exhibit a low C:N ratio in winter high flow period and higher C:N ratio during low flow period. The N:P ratio in these catchments will be high during the low flow periods (high NO₃ and low SRP concentrations). Catchments where DOC-NO₃ variations are out-of-phase with discharge will exhibit probably less variation in their ratios (because of lower NO₃ amplitude) with relatively higher winter C:N ratio than the previous type of catchments.

However, we can stress that monitoring C-N and P is important as each of these elements can follow a specific pattern, even in neighboring catchments. Yet, these three basic elements are not always analyzed in water quality monitoring. Therefore, sample points for which monitoring associate these three elements have to be preserve for a long term monitoring. They will be necessary to further investigate their variations in relation with geomorphological and climate conditions.

In this paper, we used inter-annual mean values for DOC, NO₃ and SRP loads to establish the spatial variability and the seasonal patterns across headwater catchments. Because we demonstrated that seasonality index (SI) and flow flashiness (W₂) are linked, our results can be used to classify non-monitored catchments as a function of their potential load flashiness. Flow flashiness (W₂) combined with SI or the slope of C-Q relationships for high flows, could be employed for a sampling monitoring design to improve annual or seasonal load estimations for the most contributive catchments (Moatar et al, 2020). Yet, other issues, such as the assessment of eutrophication risk for some lakes, estuaries or bays around the peninsula would require more frequent sampling especially for SRP.

5 Conclusion

To analyze spatial variability in water quality at a regional scale, we used an original dataset from public databases, little used by the scientific community, for the French region of Brittany with monthly measurements of water quality. The dataset selected covers 185 headwater and agricultural catchments monitored over a period sufficiently long (10 years) to allow the spatial (regional) variability and temporal (seasonal) variation in DOC, NO₃, and SRP concentrations to be analyzed. We described spatio-temporal variations in concentrations, loads, and seasonal patterns and analyzed their correlations with geographic variables (related to topography, hydro-climate, geology, soils, land uses, and human pressures). Our study showed the following:

- 1) Seasonal cycles of DOC and NO₃ concentrations are usually opposite from each other. Catchments with a low base-flow index exhibit maximum NO₃ in-phase with maximum flow, while those with a higher base-flow index exhibit maximum NO₃ after maximum flow. Both types exhibited maximum DOC in autumn, at the beginning of the annual increase in flow.
- 2) NO₃ concentrations increased as human pressures and base flow contribution increased. DOC concentrations decreased as rainfall, base flow contribution, and elevation increased. SRP concentrations showed weaker correlations with human pressures, rainfall, and hydrological and topographic variables.
- 3) Seasonal SRP cycles are synchronized in nearly all catchments that have a clear seasonal amplitude, with maximum SRP concentrations that occur during the summer low-flow period due to a decreased dilution capacity of point sources.

The spatial and temporal opposition between DOC and NO₃ concentrations likely results from a combination of heterogeneous human inputs and biogeochemical connection between these pools. The seasonal cycles in stream concentrations result from the mixing of water parcels that followed contrasting flowpaths, combined with high spatial variability in nutrient sources, local-scale biogeochemical processes, and point sources. As a perspective, we recommend further studies of multiple elements that are likely to show contrasting responses to diverse human pressures and to the retention/removal capacities of hydrosystems.

Acknowledgments

The salary of SG was supported by Region Bretagne and Agence de l'Eau Loire Bretagne. We thanks Dr Remi Dupas (INRAE
595 Rennes) for his valuable contribution for methodological choices and the scientific interpretations and discussions. We thank
Dr Vazken Andreassian (INRAE Anthony) for providing regional simulations of discharge time series with the model GR4J.
We thank also Josette Launay (CRESEB), Elodie Bardon (Observatoire Environnement Bretagne), Yves-Marie Heno and
Olivier Nauleau (DREAL Bretagne) for their contributions to the data selection and to the project. Finally, we thanks all the
people who contributed to the collection of public data on surface water quality in French Brittany.

600 References

- Abbott, B. W., Gruau, G., Zarnetske, J. P., Moatar, F., Barbe, L., Thomas, Z., Fovet, O., Kolbe, T., Gu, S., Pierson-
Wickmann, A.-C., Davy, P., and Pinay, G.: Unexpected spatial stability of water chemistry in headwater stream
networks, *Ecol. Lett.*, 21, 296-308, <https://doi.org/10.1111/ele.12897>, 2018a.
- Abbott, B. W., Moatar, F., Gauthier, O., Fovet, O., Antoine, V., and Ragueneau, O.: Trends and seasonality of river nutrients
605 in agricultural catchments: 18 years of weekly citizen science in France, *Sci. Total Environ.*, 624, 845-858,
<https://doi.org/10.1016/j.scitotenv.2017.12.176>, 2018b.
- Ågren, A., Buffam, I., Jansson, M., and Laudon, H.: Importance of seasonality and small streams for the landscape regulation
of dissolved organic carbon export, *J. Geophys. Res.-Biogeo.*, 112, <https://doi.org/10.1029/2006JG000381>, 2007.
- Alexander, R. B., Boyer, E. W., Smith, R. A., Schwarz, G. E., and Moore, R. B.: The Role of Headwater Streams in
610 Downstream Water Quality, *J Am Water Resour Assoc*, 43, 41-59, [10.1111/j.1752-1688.2007.00005.x](https://doi.org/10.1111/j.1752-1688.2007.00005.x), 2007.
- Andersson, J.-O. and Nyberg, L.: Spatial variation of wetlands and flux of dissolved organic carbon in boreal headwater
streams, *Hydrol. Process.*, 22, 1965-1975, <https://doi.org/10.1002/hyp.6779>, 2008.
- Aubert, A. H., Gascuel-Oudou, C., Gruau, G., Akkal, N., Fauchoux, M., Fauvel, Y., Grimaldi, C., Hamon, Y., Jaffrézic, A.,
Lecoz-Boutnik, M., Molénat, J., Petitjean, P., Ruiz, L., and Merot, P.: Solute transport dynamics in small, shallow
615 groundwater-dominated agricultural catchments: insights from a high-frequency, multisolute 10 yr-long monitoring study,
Hydrol. Earth Syst. Sci., 17, 1379-1391, <https://doi.org/10.5194/hess-17-1379-2013>, 2013.
- Barnes, R. T. and Raymond, P. A.: Land-use controls on sources and processing of nitrate in small watersheds: insights from
dual isotopic analysis, *Ecol. Appl.*, 20, 1961-1978, <https://doi.org/10.1890/08-1328.1>, 2010.
- Basu, N. B., Destouni, G., Jawitz, J. W., Thompson, S. E., Loukinova, N. V., Darracq, A., Zanardo, S., Yaeger, M., Sivapalan,
620 M., Rinaldo, A., and Rao, P. S. C.: Nutrient loads exported from managed catchments reveal emergent biogeochemical
stationarity, *Geophys. Res. Lett.*, 37, <https://doi.org/10.1029/2010GL045168>, 2010.
- Basu, N. B., Thompson, S. E., and Rao, P. S. C.: Hydrologic and biogeochemical functioning of intensively managed
catchments: A synthesis of top-down analyses, *Water Resources Research*, 47, <https://doi.org/10.1029/2011WR010800>,
2011.

- 625 Beven, K. J. and Kirkby, M. J.: A physically based, variable contributing area model of basin hydrology / Un modèle à base physique de zone d'appel variable de l'hydrologie du bassin versant, *Hydrological Sciences Bulletin*, 24, 43-69, <https://doi.org/10.1080/02626667909491834>, 1979.
- Bishop, K., Buffam, I., Erlandsson, M., Fölster, J., Laudon, H., Seibert, J., and Temnerud, J.: *Aqua Incognita: the unknown headwaters*, *Hydrol. Process.*, 22, 1239-1242, <https://doi.org/10.1002/hyp.7049>, 2008.
- 630 Bol, R., Gruau, G., Mellander, P.-E., Dupas, R., Bechmann, M., Skarbøvik, E., Bieroza, M., Djodjic, F., Glendell, M., Jordan, P., Van der Grift, B., Rode, M., Smolders, E., Verbeeck, M., Gu, S., Klumpp, E., Pohle, I., Fresne, M., and Gascuel-Oudou, C.: Challenges of reducing phosphorus based water eutrophication in the agricultural landscapes of northwest Europe, *Front. Mar. Sci.*, 5, <https://doi.org/10.3389/fmars.2018.00276>, 2018.
- Bowes, M. J., Jarvie, H. P., Halliday, S. J., Skeffington, R. A., Wade, A. J., Loewenthal, M., Gozzard, E., Newman, J. R., and
635 Palmer-Felgate, E. J.: Characterising phosphorus and nitrate inputs to a rural river using high-frequency concentration–flow relationships, *Sci. Total Environ.*, 511, 608-620, <https://doi.org/10.1016/j.scitotenv.2014.12.086>, 2015.
- Bowes, M. J., Smith, J. T., Neal, C., Leach, D. V., Scarlett, P. M., Wickham, H. D., Harman, S. A., Armstrong, L. K., Davy-Bowker, J., Haft, M., and Davies, C. E.: Changes in water quality of the River Frome (UK) from 1965 to 2009: Is phosphorus mitigation finally working?, *Sci. Total Environ.*, 409, 3418-3430,
640 <https://doi.org/10.1016/j.scitotenv.2011.04.049>, 2011.
- Brooks, P. D., McKnight, D. M., and Bencala, K. E.: The relationship between soil heterotrophic activity, soil dissolved organic carbon (DOC) leachate, and catchment-scale DOC export in headwater catchments, *Water Resour. Res.*, 35, 1895-1902, <https://doi.org/10.1029/1998WR900125>, 1999.
- Colmar, A., Walter, C., Le Bissonnais, Y., and Daroussin, J.: Démarche de validation régionale par avis d'experts du modèle
645 MESALES d'estimation de l'aléa érosif, *Etude et Gestion des Sols*, 17, 19-32, 2010.
- Cooper, R. J., Rawlins, B. G., Krueger, T., Lézé, B., Hiscock, K. M., and Pedentchouk, N.: Contrasting controls on the phosphorus concentration of suspended particulate matter under baseflow and storm event conditions in agricultural headwater streams, *Sci. Total Environ.*, 533, 49-59, <https://doi.org/10.1016/j.scitotenv.2015.06.113>, 2015.
- Cosgrove, W. J. and Loucks, D. P.: Water management: Current and future challenges and research directions, *Water Resour. Res.*, 51, 4823-4839, <https://doi.org/10.1002/2014WR016869>, 2015.
- 650 Creed, I. F., Beall, F. D., Clair, T. A., Dillon, P. J., and Hesslein, R. H.: Predicting export of dissolved organic carbon from forested catchments in glaciated landscapes with shallow soils, *Global Biogeochem. Cy.*, 22, <https://doi.org/10.1029/2008GB003294>, 2008.
- Davidson, E. A., Janssens, I. A., and Luo, Y.: On the variability of respiration in terrestrial ecosystems: moving beyond Q10, *Global Change Biology*, 12, 154-164, <https://doi.org/10.1111/j.1365-2486.2005.01065.x>, 2006.
- 655 Dawson, J. J. C., Soulsby, C., Tetzlaff, D., Hrachowitz, M., Dunn, S. M., and Malcolm, I. A.: Influence of hydrology and seasonality on DOC exports from three contrasting upland catchments, *Biogeochemistry*, 90, 93-113, <https://doi.org/10.1007/s10533-008-9234-3>, 2008.

- Delmas, M., Saby, N., Arrouays, D., Dupas, R., Lemerrier, B., Pellerin, S., and Gascuel-Oudou, C.: Explaining and mapping
660 total phosphorus content in French topsoils, *Soil Use Manage.*, 31, 259-269, <https://doi.org/10.1111/sum.12192>, 2015.
- Dodds, W. K. and Smith, V. H.: Nitrogen, phosphorus, and eutrophication in streams, *Inland Waters*, 6, 155-164, DOI:
[10.5268/TW-6.2.909](https://doi.org/10.5268/TW-6.2.909), 2016.
- Duan, S., Kaushal, S. S., Groffman, P. M., Band, L. E., and Belt, K. T.: Phosphorus export across an urban to rural gradient in
the Chesapeake Bay watershed, *J. Geophys. Res-Bioge*, 117, <https://doi.org/10.1029/2011JG001782>, 2012.
- 665 Duncan, J. M., Band, L. E., Groffman, P. M., and Bernhardt, E. S.: Mechanisms driving the seasonality of catchment scale
nitrate export: Evidence for riparian ecohydrologic controls, *Water Resour. Res.*, 51, 3982-3997,
<https://doi.org/10.1002/2015WR016937>, 2015.
- Dupas, R., Delmas, M., Dorioz, J.-M., Garnier, J., Moatar, F., and Gascuel-Oudou, C.: Assessing the impact of agricultural
pressures on N and P loads and eutrophication risk, *Ecol. Indic.*, 48, 396-407,
670 <https://doi.org/10.1016/j.ecolind.2014.08.007>, 2015a.
- Dupas, R., Gruau, G., Gu, S., Humbert, G., Jaffrézic, A., and Gascuel-Oudou, C.: Groundwater control of biogeochemical
processes causing phosphorus release from riparian wetlands, *Water Res.*, 84, 307-314,
<https://doi.org/10.1016/j.watres.2015.07.048>, 2015b.
- Dupas, R., Minaudo, C., and Abbott, B. W.: Stability of spatial patterns in water chemistry across temperate ecoregions,
675 *Environ. Res. Lett.*, 14, 074015, <https://doi.org/10.1088/1748-9326/ab24f4>, 2019.
- Dupas, R., Minaudo, C., Gruau, G., Ruiz, L., and Gascuel-Oudou, C.: Multidecadal Trajectory of Riverine Nitrogen and
Phosphorus Dynamics in Rural Catchments, *Water Resour. Res.*, 54, 5327– 5340, <https://doi.org/10.1029/2018WR022905>,
2018.
- Dupas, R., Musolff, A., Jawitz, J. W., Rao, P. S. C., Jäger, C. G., Fleckenstein, J. H., Rode, M., and Borchardt, D.: Carbon and
680 nutrient export regimes from headwater catchments to downstream reaches, *Biogeosciences*, 14, 4391-4407,
<https://doi.org/10.5194/bg-14-4391-2017>, 2017.
- Edwards, A. C., Cook, Y., Smart, R., and Wade, A. J.: Concentrations of nitrogen and phosphorus in streams draining the
mixed land-use Dee Catchment, north-east Scotland, *J. Appl. Ecol.*, 37, 159-170, <https://doi.org/10.1046/j.1365-2664.2000.00500.x>, 2000.
- 685 Evans, C. D., Reynolds, B., Jenkins, A., Helliwell, R. C., Curtis, C. J., Goodale, C. L., Ferrier, R. C., Emmett, B. A., Pilkington,
M. G., Caporn, S. J. M., Carroll, J. A., Norris, D., Davies, J., and Coull, M. C.: Evidence that Soil Carbon Pool Determines
Susceptibility of Semi-Natural Ecosystems to Elevated Nitrogen Leaching, *Ecosystems*, 9, 453-462,
<https://doi.org/10.1007/s10021-006-0051-z>, 2006.
- Exner-Kittridge, M., Strauss, P., Blöschl, G., Eder, A., Saracevic, E., and Zessner, M.: The seasonal dynamics of the stream
690 sources and input flow paths of water and nitrogen of an Austrian headwater agricultural catchment, *Sci. Total Environ.*,
542, 935-945, <https://doi.org/10.1016/j.scitotenv.2015.10.151>, 2016.

- 695 FAO and WWC: Towards a water and food secure future: Critical perspectives for policy-makers, Food and Agriculture
 Organization of the United Nations (FAO) and the World Water Council (WWC) in support to the High Level Panel on
 Water for Food Security, Seventh World Water Forum in Daegu, South Korea, White paper, 76 pp., [http://www.fao.org/3/a-
 i4560e.pdf](http://www.fao.org/3/a-i4560e.pdf), 2015.
- Fasching, C., Ulseth, A. J., Schelker, J., Steniczka, G., and Battin, T. J.: Hydrology controls dissolved organic matter export
 and composition in an Alpine stream and its hyporheic zone, *Limnol. Oceanogr.*, 61, 558-571,
<https://doi.org/10.1002/lno.10232>, 2016.
- 700 Fasching, C., Wilson, H. F., D'Amario, S. C., and Xenopoulos, M. A.: Natural Land Cover in Agricultural Catchments Alters
 Flood Effects on DOM Composition and Decreases Nutrient Levels in Streams, *Ecosystems*, 22, 1530-1545,
<https://doi.org/10.1007/s10021-019-00354-0>, 2019.
- Findlay, S. E.: Increased carbon transport in the Hudson River: unexpected consequence of nitrogen deposition?, *Front. Ecol.
 Environ.*, 3, 133-137, [https://doi.org/10.1890/1540-9295\(2005\)003\[0133:ICTITH\]2.0.CO;2](https://doi.org/10.1890/1540-9295(2005)003[0133:ICTITH]2.0.CO;2), 2005.
- 705 Gardner, K. K. and McGlynn, B. L.: Seasonality in spatial variability and influence of land use/land cover and watershed
 characteristics on stream water nitrate concentrations in a developing watershed in the Rocky Mountain West: Human
 impacts on spatial N patterns, *Water Resour. Res.*, 45, <https://doi.org/10.1029/2008WR007029>, 2009.
- Goodale, C. L., Aber, J. D., Vitousek, P. M., and McDowell, W. H.: Long-term decreases in stream nitrate: successional causes
 unlikely; possible links to DOC?, *Ecosystems*, 8, 334-337, <https://doi.org/10.1007/s10021-003-0162-8>, 2005.
- 710 Graeber, D., Gelbrecht, J., Pusch, M. T., Anlanger, C., and von Schiller, D.: Agriculture has changed the amount and
 composition of dissolved organic matter in Central European headwater streams, *Sci. Total Environ.*, 438, 435-446,
<https://doi.org/10.1016/j.scitotenv.2012.08.087>, 2012.
- Griffiths, N. A., Tank, J. L., Royer, T. V., Warrner, T. J., Frauendorf, T. C., Rosi-Marshall, E. J., and Whiles, M. R.: Temporal
 variation in organic carbon spiraling in Midwestern agricultural streams, *Biogeochemistry*, 108, 149-169,
<https://doi.org/10.1007/s10533-011-9585-z>, 2011.
- 715 Grizzetti, B., Bouraoui, F., de Marsily, G., and Bidoglio, G.: A statistical method for source apportionment of riverine nitrogen
 loads, *J. Hydrol.*, 304, 302-315, <https://doi.org/10.1016/j.jhydrol.2004.07.036>, 2005.
- Grolemund, G. and Wickham, H.: Dates and Times Made Easy with lubridate, *Journal of Statistical Software*, 40, 1-25, DOI:
[10.18637/jss.v040.i03](https://doi.org/10.18637/jss.v040.i03), 2011.
- 720 Gu, S., Gruau, G., Dupas, R., Petitjean, P., Li, Q., and Pinay, G.: Respective roles of Fe-oxyhydroxide dissolution, pH changes
 and sediment inputs in dissolved phosphorus release from wetland soils under anoxic conditions, *Geoderma*, 338, 365-374,
<https://doi.org/10.1016/j.geoderma.2018.12.034>, 2019.
- 725 Gu, S., Gruau, G., Dupas, R., Rumpel, C., Crème, A., Fovet, O., Gascuel-Oudou, C., Jeanneau, L., Humbert, G., and Petitjean,
 P.: Release of dissolved phosphorus from riparian wetlands: Evidence for complex interactions among hydroclimate
 variability, topography and soil properties, *Sci. Total Environ.*, 598, 421-431,
<https://doi.org/10.1016/j.scitotenv.2017.04.028>, 2017.

- Gücker, B., Silva, R. C. S., Graeber, D., Monteiro, J. A. F., and Boëchat, I. G.: Urbanization and agriculture increase exports and differentially alter elemental stoichiometry of dissolved organic matter (DOM) from tropical catchments, *Sci. Total Environ.*, 550, 785-792, <https://doi.org/10.1016/j.scitotenv.2016.01.158>, 2016.
- 730 Halliday, S. J., Wade, A. J., Skeffington, R. A., Neal, C., Reynolds, B., Rowland, P., Neal, M., and Norris, D.: An analysis of long-term trends, seasonality and short-term dynamics in water quality data from Plynlimon, Wales, *Sci. Total Environ.*, 434, 186-200, <https://doi.org/10.1016/j.scitotenv.2011.10.052>, 2012.
- Hedin, L. O., von Fischer, J. C., Ostrom, N. E., Kennedy, B. P., Brown, M. G., and Robertson, G. P.: Thermodynamic Constraints on Nitrogen Transformations and Other Biogeochemical Processes at Soil-Stream Interfaces, *Ecology*, 79, 684-703, DOI: 10.2307/176963, 1998.
- 735 Hénault, C. and Germon, J. C.: NEMIS, a predictive model of denitrification on the field scale, *European Journal of Soil Science*, 51, 257-270, <https://doi.org/10.1046/j.1365-2389.2000.00314.x>, 2000.
- Heppell, C. M., Binley, A., Trimmer, M., Darch, T., Jones, A., Malone, E., Collins, A. L., Johnes, P. J., Freer, J. E., and Lloyd, C. E. M.: Hydrological controls on DOC : nitrate resource stoichiometry in a lowland, agricultural catchment, southern UK, *Hydrol. Earth Syst. Sc.*, 21, 4785-4802, <https://doi.org/10.5194/hess-21-4785-2017>, 2017.
- 740 Hill, A. R., Devito, K. J., Campagnolo, S., and Sanmugadas, K.: Subsurface denitrification in a forest riparianzone: Interactions between hydrology and supplies of nitrate and organic carbon, *Biogeochemistry*, 51, 193-223, <https://doi.org/10.1023/A:1006476514038>, 2000.
- Humbert, G., Jaffrézic, A., Fovet, O., Gruau, G., and Durand, P.: Dry-season length and runoff control annual variability in stream DOC dynamics in a small, shallowgroundwater-dominated agricultural watershed, *Water Resour. Res.*, 51, 7860-7877, <https://doi.org/10.1002/2015WR017336>, 2015.
- 745 Hytteborn, J. K., Temnerud, J., Alexander, R. B., Boyer, E. W., Futter, M. N., Fröberg, M., Dahné, J., and Bishop, K. H.: Patterns and predictability in the intra-annual organic carbon variability across the boreal and hemiboreal landscape, *Sci. Total Environ.*, 520, 260-269, <https://doi.org/10.1016/j.scitotenv.2015.03.041>, 2015.
- Kaushal, S. S., Gold, A. J., Bernal, S., Johnson, T. A. N., Addy, K., Burgin, A., Burns, D. A., Coble, A. A., Hood, E., Lu, Y., Mayer, P., Minor, E. C., Schroth, A. W., Vidon, P., Wilson, H., Xenopoulos, M. A., Doody, T., Galella, J. G., Goodling, P., Haviland, K., Haq, S., Wessel, B., Wood, K. L., Jaworski, N., and Belt, K. T.: Watershed 'chemical cocktails': forming novel elemental combinations in Anthropocene fresh waters, *Biogeochemistry*, 141, 281-305, <https://doi.org/10.1007/s10533-018-0502-6>, 2018.
- 750 Lambert, T., Pierson-Wickmann, A.-C., Gruau, G., Jaffrezic, A., Petitjean, P., Thibault, J.-N., and Jeanneau, L.: Hydrologically driven seasonal changes in the sources and production mechanisms of dissolved organic carbon in a small lowland catchment, *Water Resour. Res.*, 49, 5792-5803, <https://doi.org/10.1002/wrcr.20466>, 2013.
- 755 Le, S., Josse, J., and Husson, F.: FactoMineR: An R Package for Multivariate Analysis, *J. Stat. Softw.*, 25, 1-18, DOI: [10.18637/jss.v025.i01](https://doi.org/10.18637/jss.v025.i01), 2008.

- Lemercier, B., Gaudin, L., Walter, C., Arousseau, P., Arrouays, D., Schwartz, C., Saby, N. P. A., Follain, S., and Abrassart, J.: Soil phosphorus monitoring at the regional level by means of a soil test database, *Soil Use Manage.*, 24, 131-138, <https://doi.org/10.1111/j.1475-2743.2008.00146.x>, 2008.
- Le Moal, M., Gascuel-Oudou, C., Ménesguen, A., Souchon, Y., Étrillard, C., Levain, A., Moatar, F., Pannard, A., Souchu, P., Lefebvre, A., and Pinay, G.: Eutrophication: A new wine in an old bottle?, *Sci. Total Environ.*, 651, 1-11, <https://doi.org/10.1016/j.scitotenv.2018.09.139>, 2019.
- Lintern, A., Webb, J. A., Ryu, D., Liu, S., Bende-Michl, U., Waters, D., Leahy, P., Wilson, P., and Western, A. W.: Key factors influencing differences in stream water quality across space, *Wiley Interdisciplinary Reviews: Water*, 5, e1260, <https://doi.org/10.1002/wat2.1260>, 2018.
- Liu, W., Xu, X., McGoff, N. M., Eaton, J. M., Leahy, P., Foley, N., and Kiely, G.: Spatial and Seasonal Variation of Dissolved Organic Carbon (DOC) Concentrations in Irish Streams: Importance of Soil and Topography Characteristics, *Environmental Management*, 53, 959-967, <https://doi.org/10.1007/s00267-014-0259-1>, 2014.
- Luo, Y. and Zhou, X.: CHAPTER 5 - Controlling Factors. In: *Soil Respiration and the Environment*, Luo, Y. and Zhou, X. (Eds.), Academic Press, Burlington, <https://doi.org/10.1016/B978-012088782-8/50005-X>, 2006.
- Mardhel, V. and Gravier, A.: Carte de vulnérabilité intrinsèque simplifiée des eaux souterraines du Bassin Seine- Normandie, Report BRGM/RP54148-FR, 92 pp., 2004.
- Martin, C., Aquilina, L., Gascuel-Oudou, C., Molénat, J., Faucheux, M., and Ruiz, L.: Seasonal and interannual variations of nitrate and chloride in stream waters related to spatial and temporal patterns of groundwater concentrations in agricultural catchments, *Hydrol. Process.*, 18, 1237-1254, <https://doi.org/10.1002/hyp.1395>, 2004.
- Martin, C., Molénat, J., Gascuel-Oudou, C., Vouillamoz, J. M., Robain, H., Ruiz, L., Faucheux, M., and Aquilina, L.: Modelling the effect of physical and chemical characteristics of shallow aquifers on water and nitrate transport in small agricultural catchments, *J. Hydrol.*, 326, 25-42, <https://doi.org/10.1016/j.jhydrol.2005.10.040>, 2006.
- Melland, A. R., Mellander, P. E., Murphy, P. N. C., Wall, D. P., Mehan, S., Shine, O., Shortle, G., and Jordan, P.: Stream water quality in intensive cereal cropping catchments with regulated nutrient management, *Environ. Sci. Policy*, 24, 58-70, <https://doi.org/10.1016/j.envsci.2012.06.006>, 2012.
- Mengistu, S. G., Creed, I. F., Webster, K. L., Enanga, E., and Beall, F. D.: Searching for similarity in topographic controls on carbon, nitrogen and phosphorus export from forest headwater catchments, *Hydrol. Process.*, 28, 3201-3216, <https://doi.org/10.1002/hyp.9862>, 2014.
- Merot, P., Squvidant, H., Arousseau, P., Hefting, M., Burt, T., Maitre, V., Kruk, M., Butturini, A., Thenail, C., and Viaud, V.: Testing a climato-topographic index for predicting wetlands distribution along an European climate gradient, *Ecological Modelling*, 163, 51-71, [https://doi.org/10.1016/S0304-3800\(02\)00387-3](https://doi.org/10.1016/S0304-3800(02)00387-3), 2003.
- Minaudo, C., Dupas, R., Gascuel-Oudou, C., Roubeix, V., Danis, P.-A., and Moatar, F.: Seasonal and event-based concentration-discharge relationships to identify catchment controls on nutrient export regimes, *Adv. Water Resour.*, 131, 103379, <https://doi.org/10.1016/j.advwatres.2019.103379>, 2019.

- 795 Minaudo, C., Meybeck, M., Moatar, F., Gassama, N., and Curie, F.: Eutrophication mitigation in rivers: 30 years of trends in spatial and seasonal patterns of biogeochemistry of the Loire River (1980–2012), *Biogeosciences*, 12, 2549-2563, <https://doi.org/10.5194/bg-12-2549-2015>, 2015.
- Moatar, F., Abbott, B. W., Minaudo, C., Curie, F., and Pinay, G.: Elemental properties, hydrology, and biology interact to shape concentration-discharge curves for carbon, nutrients, sediment, and major ions, *Water Resources Research*, 53, 1270-1287, <https://doi.org/10.1002/2016WR019635>, 2017.
- 800 Moatar, F., Floury, M., Gold, A. J., Meybeck, M., Renard, B., Ferréol, M., Chandesris, A., Minaudo, C., Addy, K., Piffady, J., and Pinay, G.: Stream Solutes and Particulates Export Regimes: A New Framework to Optimize Their Monitoring, *Front Ecol Evol*, 7, <https://doi.org/10.3389/fevo.2019.00516>, 2020.
- Moatar, F. and Meybeck, M.: Riverine fluxes of pollutants: Towards predictions of uncertainties by flux duration indicators, *C.R. Geosci.*, 339, 367-382, <https://doi.org/10.1016/j.crte.2007.05.001>, 2007.
- 805 Mulholland, P. J. and Hill, W. R.: Seasonal patterns in streamwater nutrient and dissolved organic carbon concentrations: Separating catchment flow path and in-stream effects, *Water Resour. Res.*, 33, 1297-1306, <https://doi.org/10.1029/97WR00490>, 1997.
- Musolff, A., Fleckenstein, J. H., Opitz, M., Büttner, O., Kumar, R., and Tittel, J.: Spatio-temporal controls of dissolved organic carbon stream water concentrations, *J. of Hydrol.*, 566, 205-215, <https://doi.org/10.1016/j.jhydrol.2018.09.011>, 2018.
- 810 Musolff, A., Selle, B., Büttner, O., Opitz, M., and Tittel, J.: Unexpected release of phosphate and organic carbon to streams linked to declining nitrogen depositions, *Global Change Biol.*, 23, 1891-1901, <https://doi.org/10.1111/gcb.13498>, 2017.
- Mutema, M., Chaplot, V., Jewitt, G., Chivenge, P., and Blöschl, G.: Annual water, sediment, nutrient, and organic carbon fluxes in river basins: A global meta-analysis as a function of scale, *Water Resour. Res.*, 51, 8949-8972, <https://doi.org/10.1002/2014WR016668>, 2015.
- 815 Onderka, M., Wrede, S., Rodný, M., Pfister, L., Hoffmann, L., and Krein, A.: Hydrogeologic and landscape controls of dissolved inorganic nitrogen (DIN) and dissolved silica (DSi) fluxes in heterogeneous catchments, *J. Hydrol.*, 450-451, 36-47, <https://doi.org/10.1016/j.jhydrol.2012.05.035>, 2012.
- Perrin, C., Michel, C., and Andréassian, V.: Improvement of a parsimonious model for streamflow simulation, *J. Hydrol.*, 279, 275-289, [https://doi.org/10.1016/S0022-1694\(03\)00225-7](https://doi.org/10.1016/S0022-1694(03)00225-7), 2003.
- 820 Plont, S., O'Donnell, B. M., Gallagher, M. T., and Hotchkiss, E. R.: Linking carbon and nitrogen spiraling in streams, *Freshw. Sci.*, 39, 126-136, <https://doi.org/10.1086/707810>, 2020.
- Poisvert, C., Curie, F., and Moatar, F.: Annual agricultural N surplus in France over a 70-year period, *Nutr. Cycl. Agroecosyst.*, 107, 63-78, <https://doi.org/10.1007/s10705-016-9814-x>, 2017.
- 825 Pregitzer, K. S., Zak, D. R., Burton, A. J., Ashby, J. A., and MacDonald, N. W.: Chronic nitrate additions dramatically increase the export of carbon and nitrogen from northern hardwood ecosystems, *Biogeochemistry*, 68, 179-197, <https://doi.org/10.1023/B:BIOG.0000025737.29546.fd>, 2004.

- Preston, S. D., Alexander, R. B., Schwarz, G. E., and Crawford, C. G.: Factors affecting stream nutrient loads: a synthesis of regional SPARROW model results for the continental United States, *J. Am. Water Resour. As.*, 47, 891-915, <https://doi.org/10.1111/j.1752-1688.2011.00577.x>, 2011.
- 830 Raymond, S., Moatar, F., Meybeck, M., and Bustillo, V.: Choosing methods for estimating dissolved and particulate riverine fluxes from monthly sampling, *Hydrolog. Sci. J.*, 58, 1326-1339, <https://doi.org/10.1080/02626667.2013.814915>, 2013.
- Saby, N. P. A., Lemerrier, B., Arrouays, D., Leménager, S., Louis, B. P., Millet, F., Schellenberger, E., Squvidant, H., Swiderski, C., Toutain, B. F. P., Walter, C., and Bardy, M.: Le programme Base de Données des Analyses de Terre (BDAT) : Bilan de 20 ans de collecte de résultats d'analyses, *Etude et Gestion des Sols*, 21, 141-150, 2015.
- 835 Sandström, S., Futter, M. N., Kyllmar, K., Bishop, K., O'Connell, D. W., and Djodjic, F.: Particulate phosphorus and suspended solids losses from small agricultural catchments: Links to stream and catchment characteristics, *Science of The Total Environment*, 711, 134616, <https://doi.org/10.1016/j.scitotenv.2019.134616>, 2020.
- Sharpley, A. N., Chapra, S. C., Wedepohl, R., Sims, J. T., Daniel, T. C., and Reddy, K. R.: Managing Agricultural Phosphorus for Protection of Surface Waters: Issues and Options, *Journal of Environmental Quality*, 23, 437-451, <https://doi.org/10.2134/jeq1994.00472425002300030006x>, 1994.
- 840 Sobota, D. J., Harrison, J. A., and Dahlgren, R. A.: Linking dissolved and particulate phosphorus export in rivers draining California's Central Valley with anthropogenic sources at the regional scale, *J. Environ. Qual.*, 40, 1290-1302, <https://doi.org/10.2134/jeq2011.0010>, 2011.
- SoeS: NOPOLU-Agri. Outil de spatialisation des pressions de l'agriculture. Méthodologie et résultats pour les surplus d'azote et les émissions des gaz à effet de serre. Campagne 2010–2011. Ministère du Développement durable et de l'Énergie, 2013.
- 845 Taylor, P. G. and Townsend, A. R.: Stoichiometric control of organic carbon-nitrate relationships from soils to the sea, *Nature*, 464, 1178-1181, <https://doi.org/10.1038/nature08985>, 2010.
- Temnerud, J. and Bishop, K.: Spatial Variation of Streamwater Chemistry in Two Swedish Boreal Catchments: Implications for Environmental Assessment, *Environ. Sci. Technol.*, 39, 1463-1469, <https://doi.org/10.1021/es040045q>, 2005.
- 850 Thomas, O., Jung, A. V., Causse, J., Louyer, M. V., Piel, S., Baurès, E., and Thomas, M. F.: Revealing organic carbon–nitrate linear relationship from UV spectra of freshwaters in agricultural environment, *Chemosphere*, 107, 115-120, <https://doi.org/10.1016/j.chemosphere.2014.03.034>, 2014.
- Thompson, S. E., Basu, N. B., Lascrain Jr., J., Aubeneau, A., and Rao, P. S. C.: Relative dominance of hydrologic versus biogeochemical factors on solute export across impact gradients, *Water Resources Research*, 47, <https://doi.org/10.1029/2010WR009605>, 2011.
- 855 UNESCO, LIWQ.: International Initiative on Water Quality: promoting scientific research, knowledge sharing, effective technology and policy approaches to improve water quality for sustainable development - UNESCO Bibliothèque Numérique, 23 pp., <https://unesdoc.unesco.org/ark:/48223/pf0000243651>, 2015.
- Van Meter, K. J., Chowdhury, S., Byrnes, D. K., and Basu, N. B.: Biogeochemical asynchrony: Ecosystem drivers of seasonal concentration regimes across the Great Lakes Basin, *Limnol. Oceanogr.*, 9999, <https://doi.org/10.1002/lno.11353>, 2019.

- 860 Weigand, S., Bol, R., Reichert, B., Graf, A., Wiekenkamp, I., Stockinger, M., Luecke, A., Tappe, W., Bogena, H., Puetz, T.,
Amelung, W., and Vereecken, H.: Spatiotemporal Analysis of Dissolved Organic Carbon and Nitrate in Waters of a
Forested Catchment Using Wavelet Analysis, *Vadose Zone J.*, 16, doi:10.2136/vzj2016.09.0077, 2017.
- Westphal, K., Musolff, A., Graeber, D., and Borchardt, D.: Controls of point and diffuse sources lowered riverine nutrient
concentrations asynchronously, thereby warping molar N:P ratios, *Environ. Res. Lett.*, 15, 104009,
865 <https://doi.org/10.1088/1748-9326/ab98b6>, 2020.
- Whitehead, P. G., Wilby, R. L., Battarbee, R. W., Kernan, M., and Wade, A. J.: A review of the potential impacts of climate
change on surface water quality, *Hydrolog. Sci. J.*, 54, 101-123, <https://doi.org/10.1623/hysj.54.1.101>, 2009.
- Wickham, H.: *ggplot2: Elegant Graphics for Data Analysis*, Springer, 2016.
- Wickham, H.: The Split-Apply-Combine Strategy for Data Analysis, *J. Stat. Softw.*, 40, 1-29, DOI: [10.18637/jss.v040.i01](https://doi.org/10.18637/jss.v040.i01),
870 2011.
- Wood, S. N.: *Generalized Additive Models: An Introduction with R*, Second Edition, Chapman and Hall/CRC, 2017.
- Zambrano-Bigiarini, M.: hydroGOF: Goodness-of-fit functions for comparison of simulated and observed hydrological time
series. R package version 0.4-0-, <https://doi.org/10.5281/zenodo.839854>~~DOI:10.5281/zenodo.839854~~, 2020.
- Zarnetske, J. P., Bouda, M., Abbott, B. W., Saiers, J., and Raymond, P. A.: Generality of Hydrologic Transport Limitation of
875 Watershed Organic Carbon Flux Across Ecoregions of the United States, *Geophysical Research Letters*, 45, 11,702-
711,711, <https://doi.org/10.1029/2018GL080005>, 2018.

Supplements for Spatio-temporal controls of C-N-P dynamics across headwater catchments of a temperate agricultural region from public data analysis

5 Stella Guillemot^{1,2}, Ophelie Fovet¹, Chantal Gascuel-Odoux¹, Gérard Gruau³, Antoine Casquin¹, Florence Curie², Camille Minaudo⁴, Laurent Strohmenger¹, and Florentina Moatar^{5,2}

¹INRAE, AGROCAMPUS OUEST/INSTITUT AGRO, UMR SAS, 35000 Rennes, France

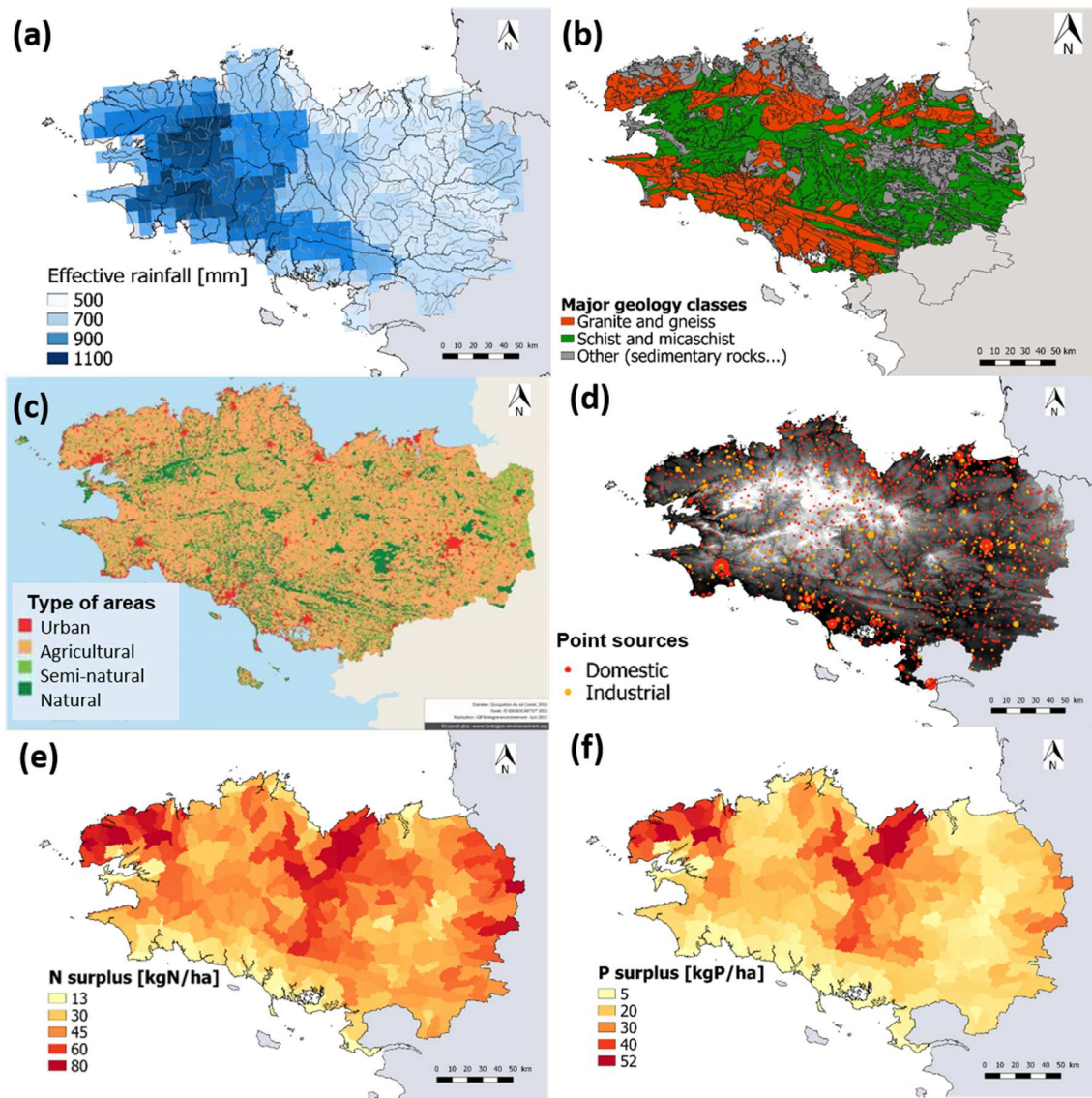
²Université de Tours, EA 6293 GéHCO, 37200 Tours, France

³OSUR, Geosciences Rennes, CNRS, Université Rennes 1, 35000 Rennes, France

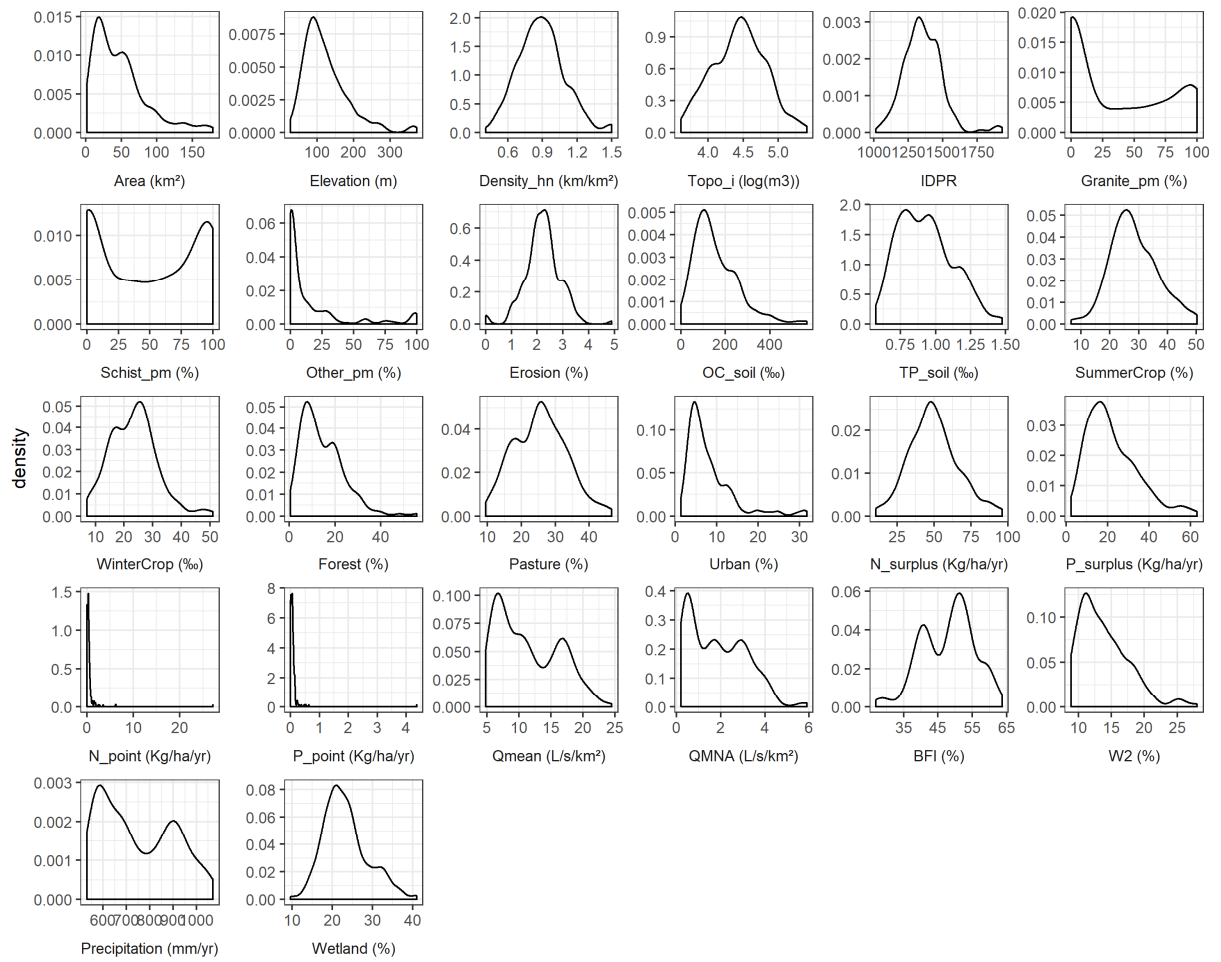
10 ⁴EPFL, Physics of Aquatic Systems Laboratory, 1015 Lausanne, Switzerland

⁵INRAE, RIVERLY, 69625 Villeurbanne, France

Correspondence to: Ophelie Fovet (ophelie.fovet@inrae.fr)



15 **Figure S1.** General characteristics of the Brittany region: (a) effective rainfall (SAFRAN database 2010), (b) geology (Sols de Bretagne database), (c) land use (OSO database), (d) nitrogen (N) and phosphorus (P) point sources (Agence de l'Eau Loire Bretagne database), (e) N surplus (NOPOLU model 2010), and (f) P surplus (NOPOLU model 2010).



20

Figure S2. Density histograms of each catchment descriptor. See Table 1 for definitions, units, and sources.

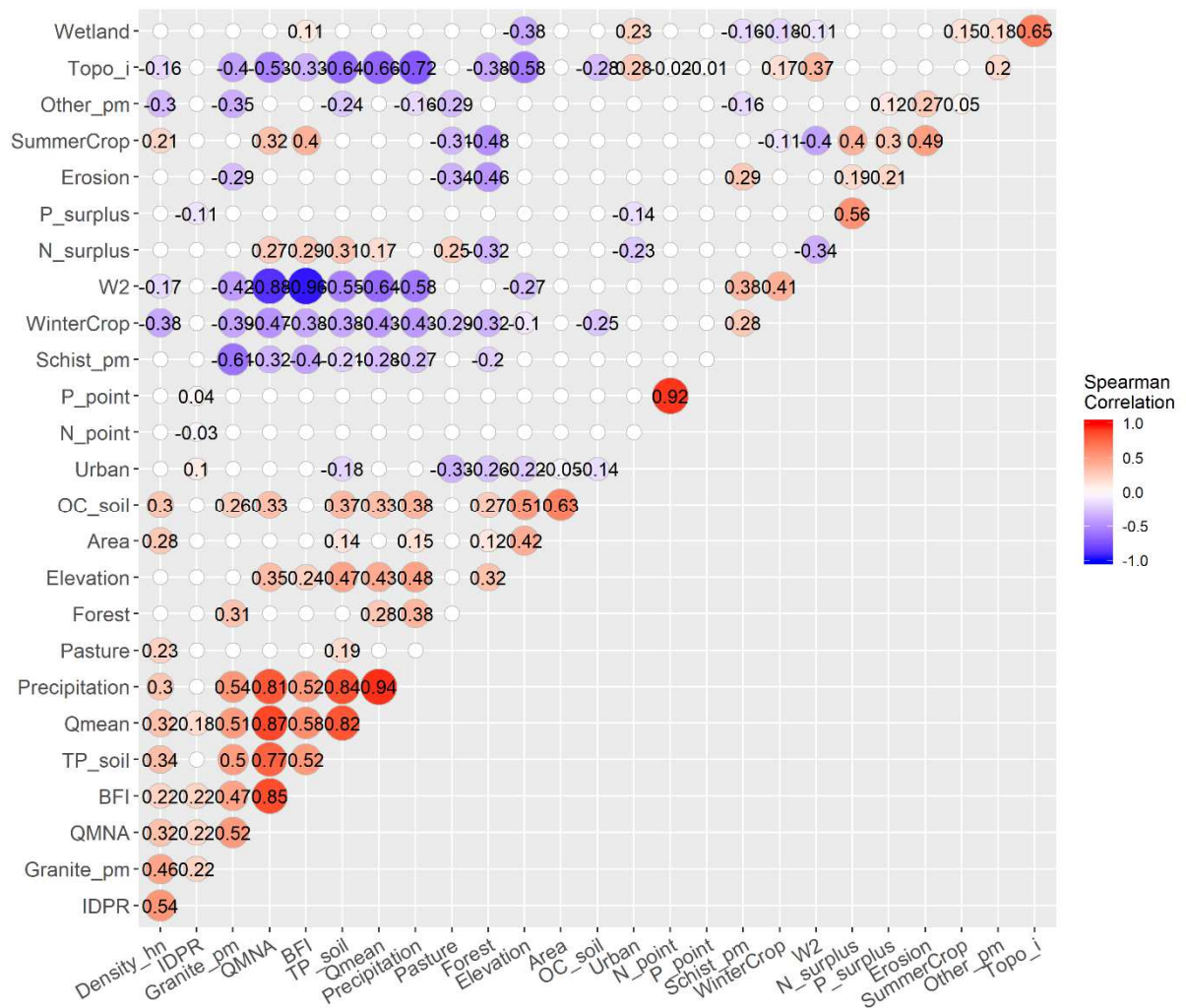
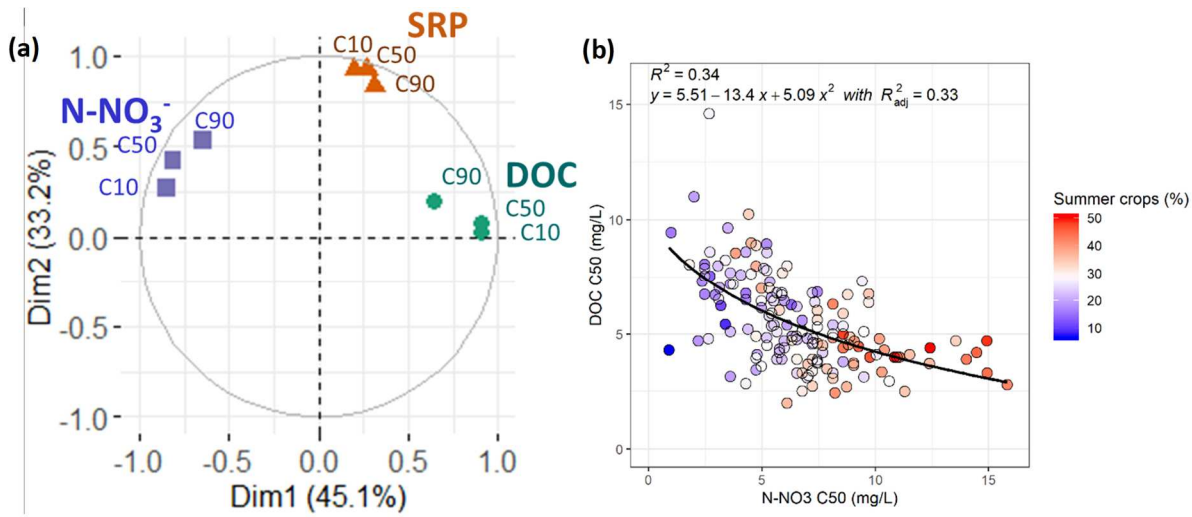
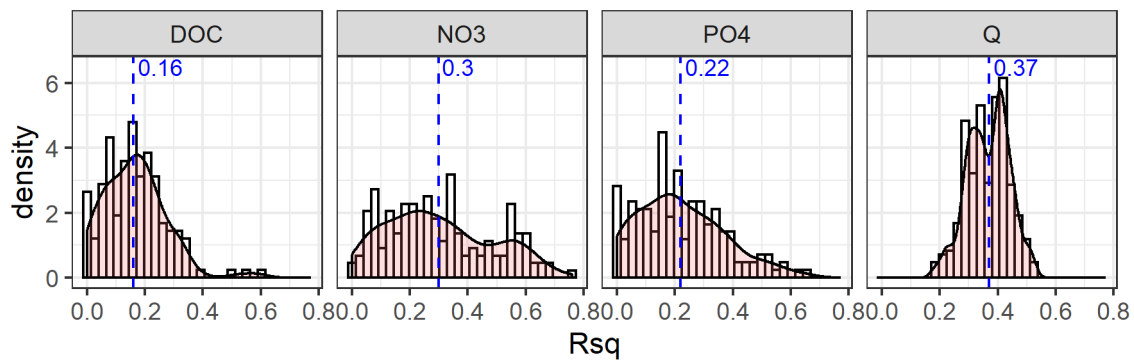


Figure S3. Correlation matrix between Headwater catchment descriptors. Spearman coefficients are visible when p-value < 0.05.

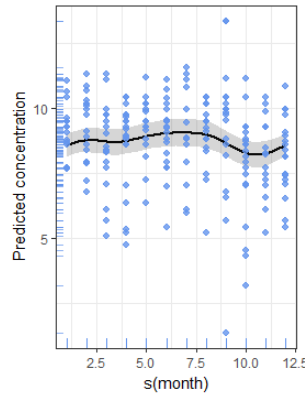


30 **Figure S4.** (a) Principal component analysis of 10th, 50th, and 90th percentiles (C10, C50 and C90) of nitrate (N-NO₃), dissolved organic carbon (DOC), and soluble reactive phosphorus (SRP) concentrations for the 185 headwater catchments analyzed; (b) Correlation between the medians (C50) of DOC and N-NO₃ concentrations for the 159 catchments in which DOC and NO₃ were monitored from 2007–2017. The color gradient indicates the percentage of catchment area covered by summer crops.

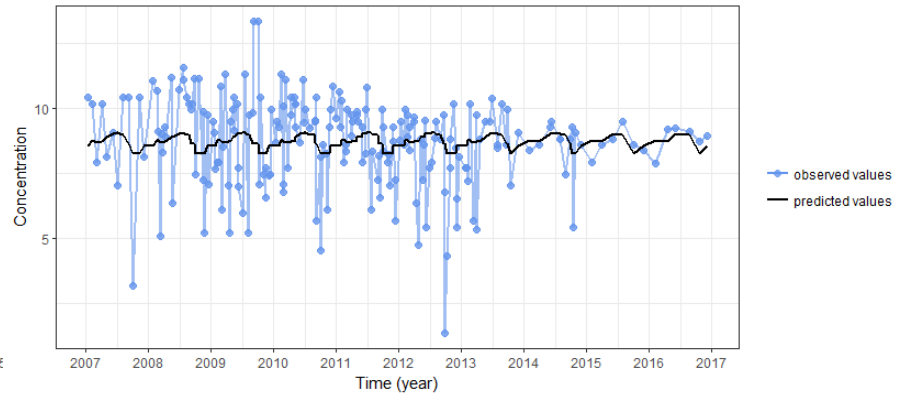


35 **Figure S45.** Density histogram of variance in the seasonal component explained by the Generalized Additive Models (GAMs) among headwater catchments for dissolved organic carbon (DOC), nitrate (NO₃), soluble reactive phosphorus (noted PO₄ here), and discharge (Q). Rsq is the coefficient of determination between observed concentrations and values calculated by the GAM. Dashed lines identify mean values.

A Seasonal GAM



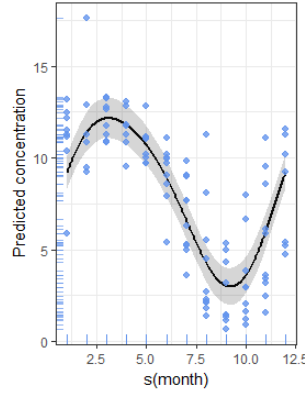
B Seasonal GAM among year – N-NO3 in mg/L – station 04162958



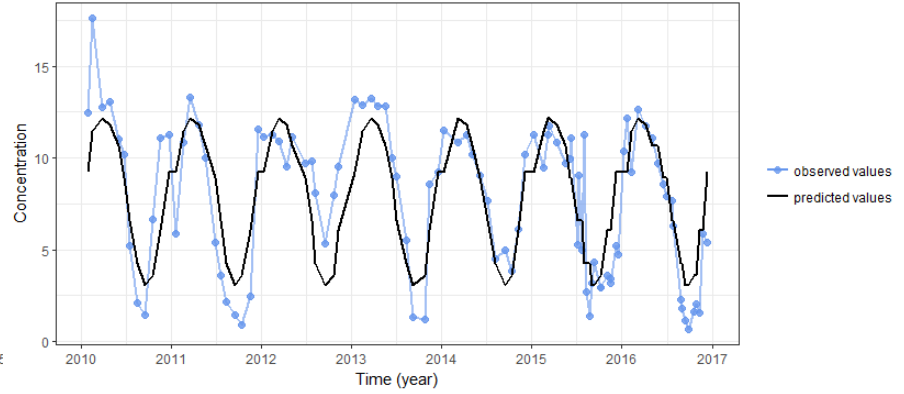
40

(1)

A Seasonal GAM



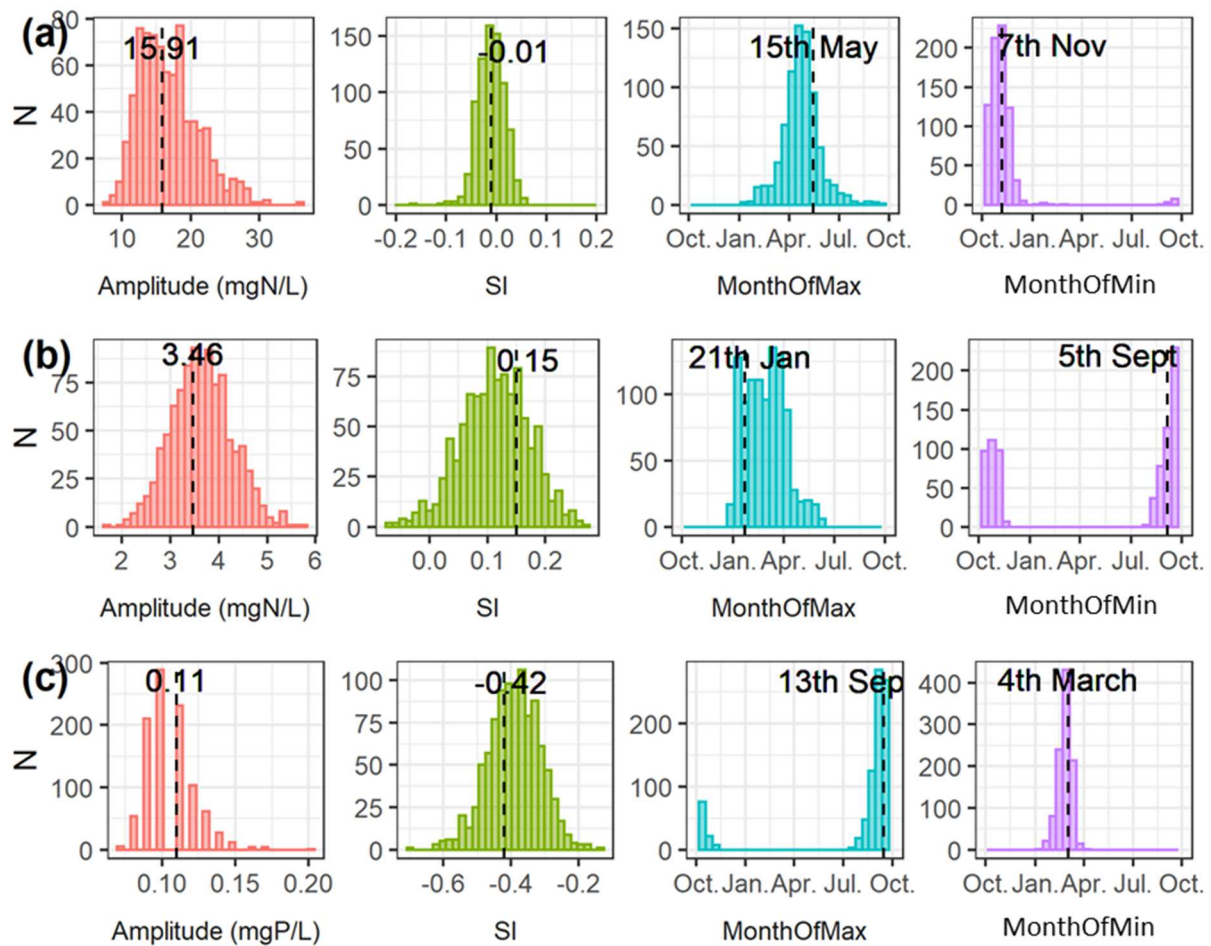
B Seasonal GAM among year – N-NO3 in mg/L – station 04191980



(2)

45

Figure S65. Two examples of Generalized Additive Model adjustments to nitrate (N-NO₃) time series: (1) La Loissance River (station no. 04162958 in the OSUR database) illustrates poor adjustment quality (Rs_q=0.02). (2) Saint Niel River/ tributary of the Blavet (station no. 04191980 in the OSUR database) illustrates good adjustment quality (Rs_q=0.66).



50 **Figure S76.** On average, the Generalized Additive Model (GAM) seasonal components were fitted to time series of monthly data,
 which is a low frequency for investigating intra-annual variations. We assumed that aggregating the 10 years would allow a relatively
 robust average seasonal pattern to be extracted. To verify this assumption, we analyzed how much the relatively low-frequency
 55 sampling influenced the seasonal metrics. We calculated differences between the seasonality indices calculated from GAMs adjusted
 to high-frequency data and those calculated from GAMs adjusted to monthly data, generated by random Monte Carlo draws
 ($n=1000$) from the high-frequency time series. This analysis was performed for three catchments Brittany for which NO_3 and SRP
 concentration data were available at higher frequency (not available for DOC data) from 2007-2016. The figure summarizes the
 variability in the seasonality indices (Ampli, seasonality index (SI), MaxPhase and MinPhase) calculated from the 1000 GAM models
 that were fitted to monthly concentration time series for (a) nitrate (NO_3) in the Kervidy-Naizin catchment, (b) NO_3 in the Néal
 60 catchment, and (c) soluble reactive phosphorus (SRP) in the Le Queffeueth catchment. Only significant GAM models ($R_{sq} \geq 0.10$)
 are shown. Dashed lines indicate the value obtained by the GAM with the original daily (Kervidy-Naizin, AgrHyS observatory) or
 weekly (Néal and Le Queffeueth catchments) time series. The y-axis corresponds to the number of catchments (N). The comparisons
 show that the distribution of seasonality metrics obtained from lower-frequency time series were centered on the values obtained
 from the original time series. Despite some delay in phases, minimum and maximum concentrations were identified during the same
 season by both types of time series. For NO_3 , the mean errors in seasonal metrics obtained from the monthly time series were -4.5%
 and 6.7% for amplitude, 21.0% and -7.2% for SI for the Kervidy-Naizin and Néal catchments respectively. PhaseMax was delayed
 65 by -1.0 to -1.5 months, and PhaseMin by 0 to 1 months. For SRP (Le Queffeueth catchment), the mean error was -4.0% for amplitude,
 -7.0% for SI, ± 18 days for PhaseMax, and ± 12 days for PhaseMin.

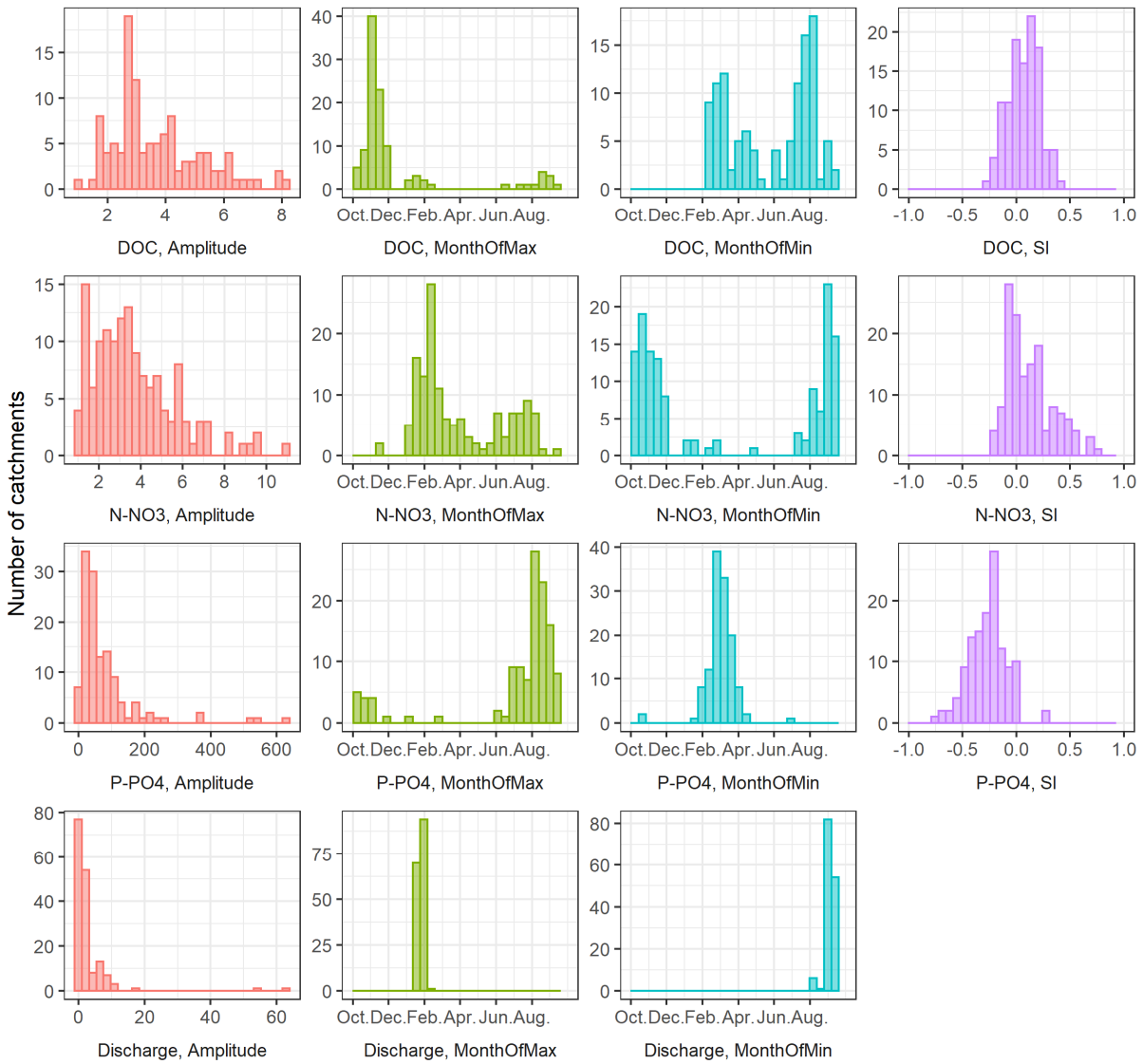
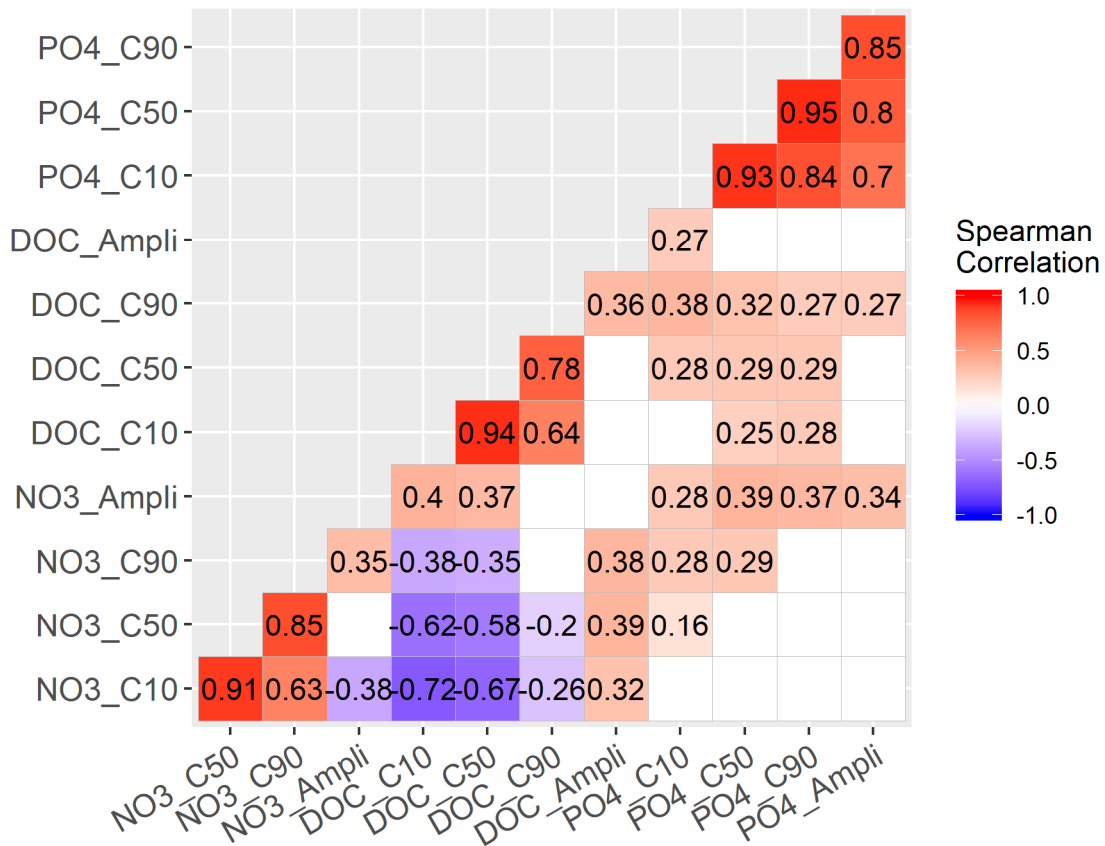


Figure S87. Histograms of water quality metrics and discharge, from left to right: absolute annual amplitude ($\text{mg}\cdot\text{l}^{-1}$), annual minimum and maximum concentration phases (in months), and the seasonal index (only for concentrations). From top to bottom: for dissolved organic carbon (DOC) ($n=113$), nitrate (N-NO_3) ($n=142$), soluble reactive phosphorus (SRP) ($n=126$), and discharge (Q) ($n=124$). Non-significant amplitudes ($R_{\text{sq}} < 0.1$) are not shown.



75

Figure S8. Matrices of Spearman's rank correlations between concentration percentiles (10th (C10), 50th (C50), and 90th (C90)) and amplitudes of dissolved organic carbon (DOC), nitrate N (noted here NO₃), and soluble reactive phosphorus (noted here PO₄). Only significant ($p < 0.05$) values are shown.